UNIVERSITY OF TRENTO

Measuring directed functional connectivity in mouse fMRI networks using Granger Causality

By

Md Taufiq Nasseef

Advisor: Prof. Stefano Panzeri

Co-Advisor: Dr. Alessandro Gozzi

Doctoral School of Cognitive and Brain Sciences

XXVIII Cycle

Thesis for the degree of Doctor of Philosophy

November, 2015

Center for Mind/Brain Sciences (CiMeC), University of Trento

Italian Institute of Technology (IIT), University of Trento

UNIVERSITY OF TRENTO

Abstract

CIMeC Center of Mind/Brain Sciences
Italian Institute of Technology

Doctor of Philosophy

Methods for measuring directed functional connectivity in mouse fMRI networks using Granger causality

By
Md Taufiq Nasseef

Resting-state functional magnetic resonance imaging (rsfMRI) of the mouse brain has revealed the presence of robust functional connectivity networks, including an antero-posterior system reminiscent of the human default network (DMN) and correlations between anterior insular and cingulate cortices recapitulating features of the human "salience network". However, rsfMRI networks are typically identified using symmetric measurements of correlation that do not provide a description of directional information flow within individual network nodes. Recent progress has allowed the measure of directed maps of functional connectivity in the human brain, providing a novel interpretative dimension that could advance our understanding of the brains' functional organization. Here, we used Granger Causality (GC), a measure of directed causation, to investigate the direction of information flow within mouse rsfMRI networks characterized by unidirectional (i.e. frontal-hippocampal) as well as reciprocal (e.g. DMN) underlying connectional architecture. We observed robust hippocampal-prefrontal dominant connectivity along the direction of projecting ventro-subicular neurons both at single subject and population level. Analysis of key DMN nodes revealed the presence of directed functional connectivity from temporal associative cortical regions to prefrontal and retrosplenial cortex, reminiscent of directional connectivity patterns described for the human DMN. We also found robust directional connectivity from insular to prefrontal areas. In a separate study, we reproduced the same directional connectivity fingerprints and showed that mice recapitulating a mutation associated to autism spectrum disorder exhibited reduced or altered directional connectivity.

Collectively, our results document converging directional connectivity towards retrosplenial and prefrontal cortical areas consistent with higher integrative functions subserved by these regions, and provide a first description of directional topology in resting-state connectivity networks that complements ongoing research in the macroscale organization of the mouse brain.

Table of Contents

List of Figures

Declaration of Authorship

I, MD TAUFIQ NASSEEF,

declare that the thesis entitled

Measuring directed functional connectivity in mouse fMRI networks using Granger Causality

and the work presented in this thesis are both my own, and have been generated by me as the result of my own original research. I confirm that:

- This work was done wholly or mainly while in candidature for a research degree at this University;
- Where any part of this thesis has previously been submitted for a degree or any other qualification at this University or any other institution, this has been clearly stated;
- Where I have consulted the published work of others, this is always clearly attributed;
- Where I have quoted from the work of others, the source is always given. With the exception of such quotations, this thesis is entirely my own work;
- I have acknowledged all main sources of help;
- Where the thesis is based on work done by myself jointly with others, I have made clear exactly what was done by others and what I have contributed myself;
- Parts of this work have been published as conference and journal papers and listed in **Appendix .**

Signed: ……

Date:…….

Acknowledgements

First and foremost I would like to express my heartiest gratitude and honour to my supervisor, Professor Stefano Panzeri for his advice, constructive criticisms and guidance. His encouragement helped in every stage of accomplishment of my PhD research work and made it much more enjoyable, and productive. He made me more critical about my ideas and thinking beyond the boundary. He is not only supervising my research work during my PhD study but also advised me to efficiently maintain work and family life balance. I would like to take the opportunity to thank my co-supervisors Alessandro Gozzi for his continuous advice and support during my course of study. I would also like to thank Adam Liska to help on my understanding of support various pre-processing steps of fMRI data. My thesis would be impossible without the financial support from SI-CODE project of the FET FP7 Programme for Research of the European Commission (under FET-Open Grant FP7284553). My special thanks to all the member of Neural Computation Lab, IIT especially Daniel Chicharro, Houman Safaai and Chamanthi Karunasekara. Also special thanks to all the members of functional neuroimaging(Fun) Lab, IIT especially Marco Pagani.

Finally, special thanks to my mother(late), father, father in law, mother in law, brother in law and my uncle for their unconditional love, understanding, great support and encouragement to pursue higher study. I also like to extend my deepest thanks to my wife for her love and support. My ultimate tribute goes to the Almighty God for bringing this work on light.

List of Abbreviations

Abbreviation	Description
1C-GC	One node conditonal Granger causality
2C-GC	Two node condtional Granger causality
ACg	Anterior cingulate cortex
AIC	Akaike information criterion
AR	Auto regression
BIC	Bayesian information criterion
BOLD	Blood oxygen level dependent
BP	Bandpass
CA1	CA1 fields of hippocampus
Cg	Cingulate cortex
CGC	Conditional Granger causality
DMN	Default mode network
DCM	Dynamic causal modelling
EEG	Electroencephalogram
EM	Expectation Maximization
FIR	Finite Impulsive Response
FT	Fourier transformation
fMRI	Functional magnetic resonance imaging
GC	Granger causality
GCCA	Granger Causal Connectivity analysis
GSR	Global signal regression
HC	Hippocampus
HRF	Hemodynamic response function
IBAAFT	Iterative Bivariate amplitude adjustment Fourier transform
ICA	Independent component analysis
IMAAFT	Iterative multivariate amplitude adjustment Fourier transform
Ins	Insular cortex
L	Left hemisphere
MEG	Magnetoencephalogram
MRI	Magnetic resonance imaging
MVAR	Multivaraite auto regression
MVGC	Multivariate Granger causality
PCA	Principle component analysis
PD	Parkinson disease
PFC	Prefrontal cortex
PCC	Posterior cingulate cortex
PCGC	Partially conditioned Granger causality
Ph fMRI	Pharmacological fMRI
PSD	Power spectral density
PWCGC	Pairwise-conditional Granger causality
PWGC	Pairwise Granger causality

PL	Prelimbric cortex
R	Right hemisphere
RsFC	Resting state functional connectivity
RsfMRI	Resting state fMRI
ROI	Region of interest
SD	Standard deviation
Rs	Retrosplenial cortex
SCA	Seed-based analysis
SN	Salience network
SNR	Signal-noise-ratio
SEM	Structural Equation Modelling
CSF	Cerebrospinal fluid
TeA	Temporal association cortex
tSNR	Temporal signal to noise ratio
VAR	Vector autoregressive
vHC	Ventral hippocampus

Chapter 1 : **Introduction**

1.1. Background

Brain function is believed to reflect the coordinated engagement of two seemingly competing processes (Friston 2011)(Lang et al. 2012): functional segregation (stating that specific functions are at least in part localized in specific areas of the brain) and functional integration (stating that complex brain function ultimately require the integration and converge of information and specific functions of individual networks).

Over the past two decades, a number of neuroimaging techniques permitting non-invasive measurements of massed neural activity from individual regions of the brain (Logothetis 2008) have emerged as crucial tools to study the functional topology of the brain and the elusive boundary between functional segregation functional integration. The use of functional and diffusion-weighted Magnetic Resonance Imaging (MRI) (Ogawa et al. 2000) in particular has provided important insights into the large-scale connectional organization of the brain and its derangement in health and pathological states. The success of this technique lies in its widespread availability, ease of use, non-invasiveness, and ability to describe non-invasively and three dimensionally brain functional and morph anatomical features on a (sub)mill metric scale.

To understand brain networks and their connectional organization both –MRI-based structural and functional connectivity have been applied. Functional connectivity mapping at-rest, termed resting-state fMRI (rsfMRI) has highlighted the presence of spatially-correlated spontaneous signal oscillations exhibiting regional specificity which define distributed networks plausibly serving as functional integrators during cognitive tasks and function. A

number of reproducible networks have been reliably described in human rsfMRI studies, including the cortical somatosensory (Biswal et al.), visual (Cordes et al. 2000)and auditory systems (Cordes et al. 2000), the salience network as well as previously characterised subcortical systems such as the basal ganglia (Hacker et al. 2013) and thalamus(Zhang et al. 2008).

Of special interest is the default mode network (DMN) (Sforazzini et al. 2014b), a prototypical distributed rsfMRI network (Seeley et al. 2007)which exhibits strong correlations in the absence of explicit tasks (i.e. at rest) and deactivates during active cognitive task. Much of the interest in these large networks lies in its aberrant connectivity profile in several neuropsychiatric patient populations(Liu et al. 2012)(Mingoia et al. 2012)(Göttlich et al. 2013).

One major limitation of the initial rsfMRI approaches is however related to that these networks were typically defined in correlational terms. Given that correlation measures are symmetric, they cannot determine the direction of communication among two correlated areas. Consequently, the initial rsfMRI results were yet unable to unravel the direction of flow of information within the default mode network. Recently, the attention in the rsfMRI field is turning to the development of computational methods that may enable to estimate and describe these networks in directional terms, a readout often referred to as "effective connectivity"(Gautama et al. 2003; Goebel et al. 2003; Ancona et al. 2004; Roebroeck et al. 2005; Ding et al. 2006; Honey et al. 2007; Nalatore et al. 2007; Marinazzo et al. 2008; Zhuang et al. 2008; Liao et al. 2009; Zhou et al. 2009, 2011; Penke and Deary 2010; Deshpande et al. 2010; Vesna Vuksanovic, Mario Bartolo, Dave Hunter 2011; W. Liao, D. Marinazzo, Z. Pan 2011; Barnett and Seth 2011, 2014; Amblard and Michel 2012; Deshpande and Hu 2012; Detto et al. 2012; Friston et al. 2014a, 2014b; Ashrafulla et al. 2013; Seth et al. 2013; Shim et al. 2013; Wen et al. 2013; Wu et al. 2013a, 2013c; Friston et

al. 2013; Hu and Liang 2014; Razi et al. 2014; Saleh 2014a). Despite the promises of this new approach, there are crucial unresolved issues that limit the inferences that can be drawn from effective connectivity rsfMRI studies. For one, the specific neuronal processes underlying spontaneous rsfMRI activity and the potential effectors of disease-related changes in rsfMRI networks (e.g. the DMN) remain undetermined, thus limiting the significance of these inferences. While there are human studies attempting to examine these issues, the multifactorial nature of these phenomena can only be disambiguated through the use of multimodal or invasive approaches in animal models.

The main objective of this thesis is to focus mainly on functional and effective connectivity, i.e. on how the neural activity in one area affects or depends upon the neural activity in other areas.

Recently, neuroimaging techniques have been coupled in animals with pharmacological manipulations (for example, pharmacological fMRI (phMRI) (Bifone and Gozzi 2011) or with genetic manipulations to study the effect of drugs, neurotransmitters and genetic factors on the communication among brain areas. phMRI-based method has proven a powerful tool to explore functional connectivity covariance networks in rodents in relation to a variety of different neurotransmitter pathways (Tononi et al. 1994; Schwarz et al. 2008; Bifone and Gozzi 2011).

More recently cortical and subcortical resting state functional connectivity(rsFC) networks composed of contralateral homologues have been reliably observed in awake and anaesthetized primates (Rilling et al. 2007; Vincent et al. 2007). A strong rationale exists for the implementation of rsfMRI also in the laboratory mouse. An extraordinarily rich repertoire of genetically modified mouse lines now exists to model the contribution of genetic alterations to the etio-pathology of various disorders of the central nervous system (Bogue

2003). Measures of directed functional connectivity in mouse models of brain pathology could be instrumental in validating this approach, and determining the neuro-pathological significance of rsFC alterations observed in analogous clinical populations. Similarly, a large collection of mouse optogenetic and pharmacogenetic tools has been recently developed to obtain cell-type specific manipulation of neuronal function with unprecedented spatio-temporal specificity(Gozzi et al. 2010). These models provide a unique experimental platform that can be used to establish causal relations between neuronal activity and effective resting-state signals, thus facilitating the investigation of the elusive neuro-physiological underpinnings of rsFC.

By employing rigorous control of motion and physiological artefacts (Ferrari et al. 2012), Alessandro Gozzi's lab and his team at the CNCS recently demonstrated the presence of robust distributed rsfMRI networks in the mouse brain(Zhan et al. 2014), including plausible homologues of the human salience and the DMN(Sforazzini et al. 2014b). Specifically, independent-component analysis (ICA) revealed inter-hemispheric homotopic rsFC networks encompassing several established neuro-anatomical systems of the mouse brain, including limbic, motor and parietal cortex, striatum, thalamus and hippocampus. Seed-based analysis confirmed the inter-hemispheric specificity of the correlations observed with ICA and highlighted the presence of distributed antero-posterior networks anatomically homologous to the human salience network (SN) and DMN. Consistent with rsFC investigations in humans, BOLD and CBV-weighted fMRI signals in the DMN-like network exhibited spontaneous anti-correlation with neighboring fronto-parietal areas. Their findings demonstrate the presence of robust distributed intrinsic functional connectivity networks in the mouse brain, and pave the way for the application of rsFC readouts in transgenic models to investigate the biological underpinnings of spontaneous BOLD fMRI fluctuations and their derangement in pathological states.

The goal of my research project is to establish and carefully validate the analytical techniques for measuring directional connectivity in mouse rsfMRI networks. When validated, the approach can be used in conjunction with genetically-manipulated mouse models to dissect the neurophysiological determinants of rsfMRI connectivity and its derangements in neuropsychiatric disorders. In the following sections, I review the concepts and tools necessary for this research endeavour.

1.2. A formal definition of structural, functional and effective connectivity

Structural connectivity refers to the presence of anatomical connections between regions, and it can be mapped to track white matter fibers reflecting the architectural infrastructure of the brain connected through polysynaptic or monosynaptic pathways of dendrites (Friston 2011)(Deshpande and Hu 2012). To complement this approach, recently functional connectivity methods have been introduced to provide statistical dependencies among remote neurophysiological events (Friston 2011)(Lang et al. 2012). Precisely, these methods rely on temporal measures, for instance, correlation, co-variance, spectral co-variance or phase locking (Lang et al. 2012) to explore important insights into functional topology of brain networks. Modern neuroimaging methods, e.g., Electroencephalogram, (EEG), Magnetoencephalogram (MEG), and MRI have successfully provided global map of the brain using both connectivity concepts.

Functional connectivity can therefore be broadly defined (Friston 2011) as statistical dependency among remote neurophysiological events. Measures of these correlations have provided important insights in rsfMRI (Sforazzini et al. 2014b)(Joel et al. 2011)(De Groof et al. 2013)(Smith 2012) . However, correlations can arise also in the absence of connections between regions because of a variety of confounding factors such as common inputs, shared neuromodulation or global covariations of activity. Thus, integration within a distributed

system is ideally better understood in terms of "effective connectivity" (Gautama et al. 2003; Goebel et al. 2003; Ancona et al. 2004; Roebroeck et al. 2005; Ding et al. 2006; Honey et al. 2007; Nalatore et al. 2007; Marinazzo et al. 2008; Zhuang et al. 2008; Liao et al. 2009; Zhou et al. 2009, 2011; Penke and Deary 2010; Deshpande et al. 2010; Vesna Vuksanovic, Mario Bartolo, Dave Hunter 2011; W. Liao, D. Marinazzo, Z. Pan 2011; Barnett and Seth 2011, 2014; Amblard and Michel 2012; Deshpande and Hu 2012; Detto et al. 2012; Friston et al. 2014a, 2014b; Ashrafulla et al. 2013; Seth et al. 2013; Shim et al. 2013; Wen et al. 2013; Wu et al. 2013a, 2013c; Friston et al. 2013; Hu and Liang 2014; Razi et al. 2014; Saleh 2014a).,a definition that refers explicitly to the influence that one neural system exerts over another. To measure effective connectivity, techniques such as Granger causality (Roebroeck et al. 2005; Ding et al. 2006; Seth 2010; Bressler and Seth 2011; Zhou et al. 2011; Deshpande and Hu 2012; Barnett and Seth 2014; Seth et al. 2015) measuring the directed effect of a neural population onto another population have been proposed (discussed below).

1.3. Functional and effective connectivity in fMRI

An important objective in brain research is to understand and describe how information dynamically propagates and link different brain regions, generating maps of brain functional connectivity [40]. Although many neuroimaging methods can be used to infer functional connectivity resting-state fMRI has been deemed one of the most popular techniques in comparison to other methods (Ashrafulla et al. 2013) because of its non- invasiveness, absence of radiation exposure, relatively wide availability, three-dimensional maps, high special resolution together with whole brain coverage (Beckmann et al. 2005)(Jolliffe 2005). RsfMRI measurements (e.g. fMRI measurements in absence of explicit tasks) detect spontaneous fluctuations in the blood oxygen level dependent (BOLD) fMRI signal and the correlational measurements that are thus generated reflect complex (and yet poorly

understood) hemodynamic oscillations that have however been shown to be tightly coupled with the underlying metabolic activity(Schwarz et al. 2008)(Bifone and Gozzi 2011).

Different computational approaches been developed to map fMRI connectivity. Indeed, this has been one of the hottest topics in computational neuroscience over the last few years. In the following, I discuss some of the most known techniques.

Seed-based analysis (SCA) is a simple bivariate measure of correlation with respect to a preselected region of interests (ROIs). This approach entails selecting ROIs and correlating the average BOLD time course of voxels within these ROIs with each other and with the time courses of all other voxels in the brain. Typically, a threshold is determined to identify voxels significantly correlated with the region of interest. A limitation (but also the main utility) of this approach is that it requires a priori selection of ROIs (Lee et al. 2013).

As an alternative to this, is to use blind source separation approaches that decompose the multivariate neural data into a set of subcomponents (or modules) than can be interpreted as indicators of the networks that tend to be co-activated over time. These decomposition techniques include independent component analysis (ICA) (Sforazzini et al. 2014b)(Joel et al. 2011)(Beckmann et al. 2005), that separates the data in a predefined number of statistically independent components, or Principal Component Analysis (PCA), that decomposes the data into a number of components that are uncorrelated (or equivalently, that are orthogonal to each other in the space of the data covariance) (Jolliffe 2005). These methods have the strength that they are hypothesis independent (as the analysis does not require the scientist to commit to any hypothesis about the ROIs involved in the network). However, they are limited by the need to select a suitable number of components, and the need to qualitatively label and classify biologically plausible networks from those reflecting noise or spurious physiological contributions. In this respect the seed approach and the blind separation

approaches are often considered complementary, and are jointly or individually used depending on the experimental question at hand.

Overall, all these standard connectivity mapping methods rely on the use of (indirect) correlations as an index of connectivity, thus preventing inferences on the topological relationship of the regions composing a network. To overcome these limitations, theoretical frameworks originally employed in neuronal electrophysiology and permitting an estimation of directed functional (effective) connectivity (e.g. the influence that one neural system exerts over another, either in the synaptic or population level (Friston 2011)) have been recently extended to rsfMRI. According to this definition, neuronal flow of information could be unidirectional (Di and Biswal 2014), bi-directional (Bitan et al. 2010) or dominant-directional (difference of directions) (Roebroeck et al. 2005). Initial applications of these approaches to explore directional connectivity in human brain networks using fMRI have produced encouraging results both in task-based (Friston et al. 2013)(Roebroeck et al. 2005) and resting state fMRI networks (Di and Biswal 2014).

1.4. How to estimate direction of effective connectivity in fMRI: model-based approaches

Efforts to ascertain causal influence from fMRI have relied primarily on mode-driven and model-free approaches such as Dynamic causal modelling (DCM) (Friston et al. 2003) and Structural Equation Modelling (SEM) (Penke and Deary 2010)(Zhuang et al. 2008). SEM, a static approach examines causal relationships by minimizing the difference between observed covariance and those have implied by a structural or path model(Penke and Deary 2010)(Zhuang et al. 2008).

DCM has been invented by Friston and colleagues(Friston et al. 2003) . It has developed to make it applicable to a variety of experimental paradigms, including task-based and resting

state protocols for almost all the neuroimaging methods (fMRI, MEG, EEG, etc.) (Friston et al. 2003, 2014c; Razi et al. 2014). Briefly, DCM fits the data to a model that includes the activity and state of the underlying neural population generating the neuroimaging signal at each location, as well as a model of the generation of the neuroimaging signal (the hemodynamic response in case of fMRI based DCM). The model fitting procedure can include prior information about the model parameters. Inversion of the model and fitting to the data is performed with a variational Bayesian technique - known as Deterministic Expectation Maximization (EM) - that evaluates the model evidence and maximizing the posterior density of the data over model parameters. Importantly for my purposes, the DCM for rsfMRI has been released as an open source toolbox that includes the generation of spontaneous activity through an autoregressive input process (a model parameter). For the rsfMRI, the generative model is estimated by specifying the probabilistic relationship between the sampling and expected cross spectra (i.e. cross-covariance, cross-spectral density, autoregression coefficients) and prior assumptions about the model structure and parameters (Razi et al. 2014)(Friston et al. 2014c). The strength of DCM is that it provides an explicit and detailed model representation of the data, and so provides all the explicit parameters of the communication pathways – including their directionality – that best explain the data. The drawback of this approach is that if the model makes wrong assumptions about the data or the dynamics of the underlying neural processes or of the hemodynamic response, then it may lead to misleading conclusions. This is a particular concern when analysing data recorded form animals, as many DCM parameters and assumptions have been fine-tuned with human fMRI data in mind.

1.5. How to estimate directed functional connectivity in fMRI: data-driven approaches

An alternative to the model-based approaches to study effective connectivity is to use approaches that are model free and try to rely only on the data and as small as possible number of assumptions. One prime example of these data-driven approaches is Granger causality (GC) (Friston et al. 2013)(Amblard and Michel 2012).

The primary idea of GC has been first described by Wiener(Wiener 1956), and later on formalized by Granger in form of linear autoregressive modelling of the stochastic processes in context of Economic theory (Ding et al. 2006). The basic idea of Wiener is very simple, and is summarized in the following in a neuroscientific language. Consider **X** and **Y** are two time series of neural activity extracted from different regions of the brain. If the knowledge of the past of **X** allows a better prediction of the current value of **Y** than the one that can be obtained simply relying on the knowledge about the past of **Y** then **X** Granger causes **Y** (Wiener 1956).

In neuroscience, Ding and colleagues has presented an expository introduction to the concept of Granger causality manipulating mathematical frameworks for both bivariate and conditional Granger causality (Ding et al. 2006). However this approach has already evidenced pragmatic for broad applications with its capability in the context of brain mapping, sensory-neural response, tracking interdependencies and researching brain disease. Vector autoregressive (VAR) modelling demonstrates crucial theory in computing Granger causality. Seth and his group has already launched two well renowned open source toolboxes under the title ‘Granger Causal Connectivity analysis (GCCA)’ (Seth 2010) and ‘Multivariate Granger Causality (MVGC)’ (Barnett and Seth 2014).

In the following, I review a number of recent mathematical advances on the calculation of GC that will be important in developing my work.

In practice, GC is often estimated by first fitting Vector autoregressive (VAR) models to the data. These are statistical models that model the next time point of a time series from a number of previous values of the time series. The number of previous time points taken into account by the VAR model is called the order of the autoregression(Barnett and Seth 2014). This is a free parameter of the analysis, and its best value is usually determined on statistical considerations such as the Akaike information criterion (AIC) and Bayesian information criterion (BIC) have been introduced to estimate best model order(Barnett and Seth 2014) (Seth 2010).

Importantly, Seth and his group recently released open source toolboxes under the title 'Granger Causal Connectivity analysis (GCCA)' (Seth 2010) and 'Multivariate Granger Causality (MVGC)' (Barnett and Seth 2014). These toolboxes allow the calculation of both GC in standard form and also important extensions such as the Pairwise-conditional Granger causality (PCGC), a new approach in which all universal variable are conditioned except bivariate pair of variables (source and sink).

The estimation of GC purely based on autoregressive models is unable to capture non-linear dependencies in the data (Hu and Liang 2014). To overcome these limitations, approaches based on non-linear regressions are currently under investigation (Ancona et al. 2004; Marinazzo et al. 2008; Liao et al. 2009; Seth 2010; W. Liao, D. Marinazzo, Z. Pan 2011; Hu and Liang 2014). A simple solution has been proposed by Seth and his group. This solution consists in fitting autoregressive coefficients of nonlinear regressions by Taylor expansions of the real data but it generally requires estimating a large number of parameters (Seth 2010). Other approaches include nonlinear kernels for instance radial basis functions (Ancona et al.

2004), geometry based reproducing Kernel Hilbert spaces (Marinazzo et al. 2008) applied in both fMRI (Liao et al. 2009) and rsfMRI (W. Liao, D. Marinazzo, Z. Pan 2011). Recently a copula based nonlinear Granger causality has been proposed to reveal high-order moment causality where condition marginal distribution has been introduced to estimate empirical conditional density by manipulating Bernstein approximation (Hu and Liang 2014).

Another important line of research has been about identifying and eliminating potential confounding effects in GC estimation from fMRI data. These factors include regression of global signal (Wu et al. 2013a), variation of Hemodynamic Response across regions (Deshpande et al. 2010)(Wen et al. 2013), low temporal sampling rate which may wash out fast neural interactions (Deshpande et al. 2010)(Wen et al. 2013)and noise (Nalatore et al. 2007)(Friston et al. 2014a)(Wen et al. 2013). GC could become unreliable when the underlying dynamics is dominated by slow (unstable) modes and in the presence of substantial measurement noise (Friston et al. 2014a). Importantly, GC of fMRI BOLD signals is invariant under hemodynamic convolution but not to downsampling (Seth et al. 2013). This implies that deconvolving the fMRI data with the hemodynamic response function to obtain an estimate of the original neural signals that gave rise to the fMRI response could actually help the estimation of GC especially in cases of low sampling rates of the fMRI signal. This deconvoluation can be performed for example using the canonical Hemodynamic Response Function (HRF) and Finite Impulsive Response (FIR) model (Wu et al. 2013a).

My goal is to take existing GC methods for measuring the directed effective connectivity[14-41] and then perform the necessary steps to validate these techniques in mice, and then discover the putative resting-state connectivity patterns. My aim is to first compare these patterns in healthy rodents to those found in higher mammals (Beckmann et al. 2005)(Fox et al. 2005)(Seeley et al. 2007), and finally to use these directed connectivity tools to understand

how the direction of information flow is perturbed in specific brain dysfunctions and diseases.

1.5. Outline of the thesis

This thesis is organized into 3 chapters. Chapter 1 contains brief review about the background, motivation, focus and goal of this thesis. Chapter 2 describes the research work done on Granger causality on resting-state fMRI mice including the results of a separate study containing group comparison between transgenic and control mice. Finally, chapter 3 draws the discussion of this thesis.

Chapter 2 **: Directional connectivity in mouse brain resting-state fMRI networks**

This chapter provides a detailed methodological account of the approach employed for directional mapping of spontaneous fMRI signals in the mouse brain, followed by a description of the main experimental findings in two independent experimental datasets, including a transgenic mouse line harbouring a mutation associated to autism spectrum disorder.

3.1 Experimental Methods

RsfMRI image acquisition and preprocessing

Imaging data were acquired in a previous study (Liska et al., 2015) and reprocessed for the purpose of this study. A short description of the experimental procedures employed is reported below. Briefly, MRI experiments were performed on male 20-24 week old C57BL/6J (B6) mice (n=41). The animal preparation protocol was recently described in great detail (Ferrari et al., 2012). Mice were anaesthetized with isoflurane (5% induction), intubated and artificially ventilated (2.5% surgery). The left femoral artery was cannulated for continuous blood pressure monitoring and blood sampling. Surgical sites were infiltrated with a non-brain penetrant local anaesthetic (Ferrari et al., 2010). At the end of surgery, isoflurane was discontinued and substituted with halothane (0.7%), an anaesthetic characterised by preserved cerebral blood flow auto-regulation (Gozzi et al., 2007). Functional data acquisition commenced 45 min after isoflurane cessation. Arterial blood gases (paCO2 and paO2) were measured at the end of the functional time series (20±5 and 257±33 mmHg, respectively). All in vivo experiments were performed using a 7.0 Tesla MRI scanner (Bruker Biospin, Milan). Transmission and reception were achieved using a 72

mm birdcage transmit coil and a saddle-shaped solenoid coil for signal reception. Single-shot BOLD rsfMRI time series were acquired using an echo planar imaging (EPI) sequence with the following parameters: TR/TE 1000/15 ms, flip angle 30°, matrix 100 × 100, field of view 2 × 2 cm2, 24 coronal slices, slice thickness 0.50 mm, 300 volumes and a total rsfMRI acquisition time of 6 min.

Image preprocessing was carried out as previously described (Sforazzini et al., 2014b). Briefly, rsfMRI time series were despiked, corrected for motion and spatially normalized to an in-house C57Bl/6J mouse brain template, head motion traces and mean ventricular signal (averaged fMRI time course within a manually-drawn ventricle mask) were regressed out of each of the time series. All rsfMRI time series were then spatially smoothed (Gaussian kernel of full width at half maximum of 0.6 mm) and band-pass filtered to a frequency window of 0.01-0.08 Hz.

Seed-based correlation maps and Granger Causality ROI location

To illustrate the anatomical distribution of the rsfMRI networks probed, and guide anatomical placement of ROI for GC analyses, seed-based correlation maps were generated using bilateral 3 × 3 × 1 voxel seeds as previously described (Sforazzini et al., 2014b). The mean rsfMRI timecourse in each seed was used to generate a whole-brain correlation map, which were then transformed into normally-distributed Z scores before assessing group level connectivity distributions using a one sample t-test. The resulting group T statistic maps were thresholded at a $Z > 3$ (ventro-hippocampal, and insular –cingulate/prefrontal network) or > 4 (DMN-like network) to highlight most prominent network features. The Z score levels employed correspond to a significance level of $p<0.0025$ and $p<0.0005$ respectively. All maps were then subject to cluster-level thresholding correction for family-wise errors, with a statistical cluster significance level $p = 0.01$ (Worsley et al., 1992).

Seed location was guided by prior investigations of distributed rsfMRI networks in mice and rats (Schwarz et al., 2013; Sforazzini et al., 2014b; Zhan et al., 2014; Sforazzini et al., 2014a)

and referred to known neuroanatomical structures based on correspondence with a mouse brain stereotaxic atlas (Paxinos and Franklin, 2003). For each probed network, seed location is reported in each of the figures overlaid on the original MRI anatomical template space using red lettering. Bilateral ventral hippocampal seeds (vHC) were selected to probe posterior the CA1/subicular areas, a region rich in direct monosynaptic projections to the medial prefrontal (prelimbic) cortex (Hoover and Vertes, 2007). These regions have been suggested to be part of the rodent homologue of the human prefrontal hippocampal network (Schwarz et al., 2013; Sforazzini et al., 2014b). Bilateral insular seeds were used to probe an insular –cingulate/prefrontal network, a neural systems that we could reliably map in anesthetized mice (Sforazzini et al., 2014b; Sforazzini et al., 2014a) and that exhibits neuroanatomical features reminiscent of a similar human brain network involved in salience attributions (Seeley et al., 2007). This networks is characterized by the presence of reciprocal axonal projections (Vertes, 2004; Hoover and Vertes, 2007; Zingg et al., 2014). To probe the directional topology of the mouse DMN, we first identified a putative DMN component ICA (15 components) as previously reported (Sforazzini et al., 2014b). The analysis highlighted a distributed network comprising prefrontal, orbital, cingulate and retrosplenial cortices, plus associative temporal cortical regions, consistent with previous rsfMRI mapping of this network (Sforazzini et al., 2014b; Liska et al., 2015). Bilateral seeds placed in temporal association cortex were used to corroborate the identified network using seed-correlation maps (Lu et al., 2012b; Sforazzini et al., 2014b). The regions belonging to the mouse DMN are characterised by complex and reciprocal axonal projections (Vertes, 2004; Hoover and Vertes, 2007; Zingg et al., 2014).

GC analysis was carried out on signal extracted on unilateral 3 × 3 × 1 voxel ROIs and processed as described below. ROI location was constrained by the spatial extension of the networks identified with seed-correlation mapping, and referred to known neuroanatomical structures based on correspondence with a mouse brain stereotaxic atlas (Paxinos and Franklin, 2004). To ensure maximal correspondence between the patterns of directional connectivity identified and the rsfMRI networks mapped, for each network, the seed-regions used for correlation mapping were also employed as unilateral ROIs in GC analysis. To ensure robustness of our directional connectivity findings within the mapped networks, multiple sets of ROIS covering different slice locations within the same rsfMRI network were probed.

Power spectral density and center frequency analysis without deconvolution

To characterize the time scales of BOLD variations in each ROI, for each subject and ROI we computed power spectral densities using Welch's method (Welch, 1967). We divided the whole recording time into Hamming windows of 256 data points with 50% overlap between windows, and we then averaged the periodograms so obtained. To estimate the typical frequency of spontaneous fMRI signal within each ROI we computed the center frequency of the periodogram as the average of frequency weighted with the ratio between the periodogram at given frequency and the sum of the periodogram across frequencies.

Granger Causality Analysis

Granger causality (GC) quantifies the extra predictive power provided by the activity of network node Y (in our case, the BOLD signal expressed in an ROI) onto the activity of a node X (in our case, the BOLD signal expressed in another ROI). In particular, the Wiener-Granger principle states that if the knowledge of the past of Y allows a better prediction of the current value of X than the one that can be obtained simply relying on the knowledge about the past of X and of any other node, then Y Granger causes X (Wiener, 1956; Granger,

1980). Accordingly, GC has been widely applied in neuroscience to characterize the directional functional connectivity between neural populations, and potentially to infer causal interactions between them (Friston et al. 2013; Chicharro and Panzeri 2014). Its applications comprise both electrophysiological recordings (Bernasconi and K+¦nig, 1999) and fMRI (Goebel et al., 2003; David et al., 2008).

A ubiquitous challenge in the estimation of Granger causality measures regards the trade-off between incorporating the maximum amount of information about the past of X and other nodes, and avoiding the curse of dimensionality, which impairs the estimation of the measures. The former is required not to overestimate the predictive power of Y, while the latter results from the necessity to estimate all the influences from time series of limited length. Bivariate Granger causality, which ignores other nodes apart from Y and X, usually leads to the false positive detection of interactions, reflected in significant nonzero values of Granger causality that are actually caused by indirect interactions or common influences of other nodes. Conditional Granger causality (Ding et al. 2006), which uses information from the past of other nodes, attenuates these effects, but can lead to a loss of statistical power for Granger causality from Y to X because the limited data may be insufficient to estimate the measures with the precision required to detect small predictability improvements due to Y after conditioning on all other nodes.

Regarding this balance between false positive detection and statistical power, several issues specific of the analysis of fMRI data should also be considered for the Granger causality principle implementation and its interpretation (Friston et al. 2013; Chicharro and Panzeri 2014). These comprise the effect of using indirect signals of neural activity (BOLD signals) and the effect of temporal aggregation due to low sampling rates, which also lead to false positive detections. Indeed, it has been shown (Roebroeck et al., 2005) that differences in the strength of GC across directions for two considered nodes are more robust to these effects

and tend to correlate more clearly to causation at the neural level. Accordingly, we here focused on the difference of GC measures across directions, instead of on the individual values themselves. As detailed below, we implement Granger causality following a modelling approach which favors the preservation of statistical power above the elimination of false positive GC values.

In its linear and most common implementation, the Granger Causality principle is tested by quantifying predictability using a vector autoregressive (VAR) model of the times series (Granger, 1969, Ding et al., 2006), and thus is intimately related to the structural analysis of VAR processes (Lütkepohl 2005). In a VAR model, the future values of the time series are determined by the past, with time lags up to p, the model order. In contrast to the original formulation of Granger causality, in which the predictive power gained by adding Y is assessed after using the (potentially) infinite past of X, in the modelling approach a finite order p is determined with some criterion to avoid the overfitting of the model. For VAR processes of finite order, the principle of Granger causality can strictly be reformulated as a set of constraints regarding the existence of nonzero coefficients in the VAR model(Sims 1972). Following this modelling approach, we started our analysis by selecting, for each subject separately, the optimal VAR model that fits together the time series of all the nodes under study. All computations were performed using the 'Multivariate Granger Causality (MVGC)' toolbox (Barnett and Seth, 2014). We determined the order of the VAR model by applying the Akaike information criterion(AIC) , see (Barnett and Seth, 2014). Subsequently, Granger causality measures were calculated varying the number of nodes used for prediction, from bivariate GC measures to conditional measures calculated from a set of four nodes.

The first step in the calculation of Granger causality from Y to X is the selection of the nodes included in the information set, i.e., the nodes which pasts is used to predict X. In general this set is formed by X, Y, and Z, where Z can be multivariate. To compute Granger causality two

autoregressive models are fitted the full model which includes Y, and the reduced model which excludes Y. The full and reduced autoregressive models of X are respectively expressed as:

$$X_t = \sum_{k=1}^{p} A_{xx,k} \cdot X_{t-k} + \sum_{k=1}^{p} A_{xy,k} \cdot Y_{t-k} + \sum_{k=1}^{p} A_{xz,k} \cdot Z_{t-k} + \varepsilon_{x,t} \quad \text{(Eq 1)}$$

$$X_t = \sum_{k=1}^{p} A'_{xx,k} \cdot X_{t-k} + \sum_{k=1}^{p} A'_{xz,k} \cdot Z_{t-k} + \varepsilon'_{x,t} \quad \text{(Eq 2)}$$

We then computed GC as the log likelihood ratio of the variance of the residuals of the full and reduced models:

$$GC = \ln \left| \frac{\Sigma'_{xx}}{\Sigma_{xx}} \right| \quad \text{(Eq 3)}$$

Where Σ_{xx} and Σ'_{xx} are the variance of the residuals of the full and reduced model respectively. Note that the order of the reduced model is constrained to be equal to the one of the full model, so that the reduced model has p degrees of freedom less. This generally leads to an overestimation of the predictability improvement with Y and thus of the magnitude GC measures. However, given that we are interested in the comparison of GC measures across directions, and considering the limited length of the time series available to fit the VAR models, this option is preferable than considering a longer past history for prediction in the reduced model, which would lead to smaller values of the GC measures, below the precision attainable from the sample size, thus rendering more difficult the comparison across directions.

The first measure we computed is the unconditional Granger Causality (abbreviated to U-GC) from node Y to node X, which considers an empty set Z. However, a drawback of this

approach is that if there is no casual influence Y to X but there are lagged dependencies of X and Y on a third variable (or group of variables Z), then a spurious causation can be reported by a measure like U-GC than does not consider Z (Wen et al., 2013; Barnett and Seth, 2015). Given that in this study we examined networks of up to four nodes, we will also calculate two variants of conditional GC (abbreviated as C-GC). The first one is denoted as 1C-GC and conditions on a single variable Z. In networks of 3 nodes, 1C-GC between two nodes was computed conditioning on the other node. In networks of 4 nodes, 1C-GC between two nodes was computed conditioning on either of the other nodes and then averaging the value over the two possible choices of conditioning nodes. In network of 4 nodes, for each pair of nodes we also examined a 2C-GC quantity, obtained conditioning over the activity of two other nodes in the network.

Given that the different GC measures are differently affected by the limited data size, we carried out simulations to evaluate their robustness and validity for a sample size comparable to the one of the experimental data. For that purpose, we chose the PFC-RS-vHC network and, for each subject, we generated time-series of varying length using the full VAR model fitted to all 4 nodes. Sample sizes were selected from 100 to 2000 data points, with steps of 100 data points. For each sample size, a total of 100 simulations were generated. For each of them, the three types of GC measures were estimated and averages across simulations of the mean and standard deviation across subjects were calculated. Furthermore, their significance was evaluated at the population level, like for the original data (see results for details of the significance analysis). In particular, averages across simulations of p-values (paired t test across subjects) were also obtained.

Finally, apart from focusing on the difference of GC values across directions, additional pre-processing steps were considered to attenuate the confounders affecting the analysis of directional functional connectivity between neural populations using fMRI data. For each

ROI, we computed the mean BOLD signal across the whole volume, and performed Granger Causality analysis between each pair of ROIs. We took advantage of recent methodological advances (Wu et al., 2013) and blindly deconvolved the fMRI time series with a canonical hemodynamic response function (HRF)(Friston et al., 1994). We used a canonical two-gamma HRF including its time-dispersion derivative to capture the effect of shift in lag of HRF due to e.g. changes in power of neural activity (Magri et al., 2012). The deconvolved time series is more closely related the underlying sequence of variations of neural activity and as such it is expected to be more sensitive to the presence or absence of directed neural interactions. In pilot computations, we computed all GC values from non-deconvolved and deconvolved time series. We verified that in the case of connectivity from ventral hippocampus to the prefrontal cortex (which is known to have a unidirectional anatomical connectivity and is thus a suitable test case for our methodology, see Results) the GC analysis from the deconvolved time series revealed much more robustly a pattern of directed connectivity reflecting axonal projections than the corresponding GC analysis based upon non-deconvolved data, suggesting that the blind HRF deconvolution increased the statistical power of the GC analysis (results not shown). After these pre-processing steps, we then computed GC for each ROI pair within specific ROI sets (i.e. network nodes) identified with seed-based correlation maps. Furthermore, to account for a potential confounding effect of non-linearity in functional signal to noise across brain regions related to the use of quadrature surface coil for rsfMRI data acquisitions, we also recomputed GC adding pink noise to the data such as to obtain a constant temporal signal-to-noise across the brain (Liska et al., 2015).

Population level significance analysis of Granger Causality

We determined the statistics of individual GC values for each node at the population level using a Student t test. However, in this study we were principally interested in evaluating, for each pair of nodes, the statistical significance of the difference between GC in the two

opposite directions. At the population level, the significance of the asymmetry in GC for a given node (i.e. the presence of directional connectivity) was computed using a Student t tests.

Subject level significance analysis of Granger Causality

To test for the existence of a direction with a predominant Granger causality value at a single subject level we used a non-parametric surrogates' construction method (Schreiber and Schmitz 2000) which allows generating surrogate time series which preserve the spectrum, cross-spectrum, and amplitude distribution of the original ones. In more detail, we used the so called Iterative Multivariate Amplitude Adjustment Fourier Transform (iMAAFT) surrogates (Schreiber and Schmitz 2000), which are generated as following: starting from a random shuffle surrogate from each of the two original time series, an iterative procedure is applied which alternates two steps, to preserve the spectrum and cross-spectrum, and the amplitude distribution, respectively. In the first step, the surrogates are Fourier-transformed and, at each frequency separately, the power coefficient is preserved while a phase shift common to both surrogates is introduced in order to randomize the phase across bands under the constraint of maintaining the relative phase differences between the two time series. In the second step, the amplitude distribution is preserved by mapping back the surrogate time series obtained from the previous step according to their amplitude rank order. This procedure is iterated until convergence.

Note that our use of the surrogates differed from their most common application (Schreiber and Schmitz 2000). Usually, the surrogates only preserve some of the properties of the original data, while other properties relevant for the measures studied (here GC) are destroyed, and the distribution of values obtained from the surrogates is compared to the value obtained from the original data that is, the surrogates are associated with a null

hypothesis against witch the original data are tested. Oppositely, in this case, since the estimation of linear Granger causality measures only relies on the covariance matrix, GC measures estimated from the original time series can be considered as a particular sample from the distribution of GC measures obtained from the surrogate data. What is tested is how compatible this distribution is with a zero difference of the GC measures in opposite directions. Significance at a given level was established non-parametrically given the percentage of generated samples that were above zero. We generated 1000 surrogates for each pair of ROIs and we selected significance at $p<0.05$, FDR corrected.

3.2 Results

Directional connectivity of hippocampal-prefrontal network

GC measures have been applied many times to neuroimaging data in an attempt to infer directed functional connections from recordings of spontaneous haemodynamic fluctuations (Deshpande et al., 2009; Liao et al., 2010) . However, GC analysis can be performed in various ways and under different computational assumptions. Attempts to validate the statistical power of these measures on real networks data with known directional connectivity remain very limited (David et al., 2008). Before applying this methodology to networks whose direction of information flow is largely unknown, we fine-tunes our GC analysis by applying it study directed connectivity within the ventro-hippocampal-prefrontal network (Fig. 2.1). This neural system is characterised by the presence of direct mono-synaptic projections from subicular/CA1 regions to prelimbic cortical areas (Hoover and Vertes 2007) that appear not to be reciprocated by direct return projection from medial prefrontal cortical areas (Hurley et al. 1991; Takagishi and Chiba 1991; Vertes 2004). The simple axonal configuration of this network suggests that, under the stationary conditions of the present work (e.g. resting-state under light anaesthesia), neural information should flow primarily from hippocampal/subicular nodes to prefrontal cortex. By investigating this network, we

could therefore assess whether directional connectivity patterns replicating mono-synaptic axonal projection can be detected under the experimental condition employed here. Specifically, we decided to evaluate the statistical power of each approach, and eventually select which approach to take, by assessing different directed functional connectivity measures against reference asymmetric connection from the hippocampus to the prefrontal cortex.

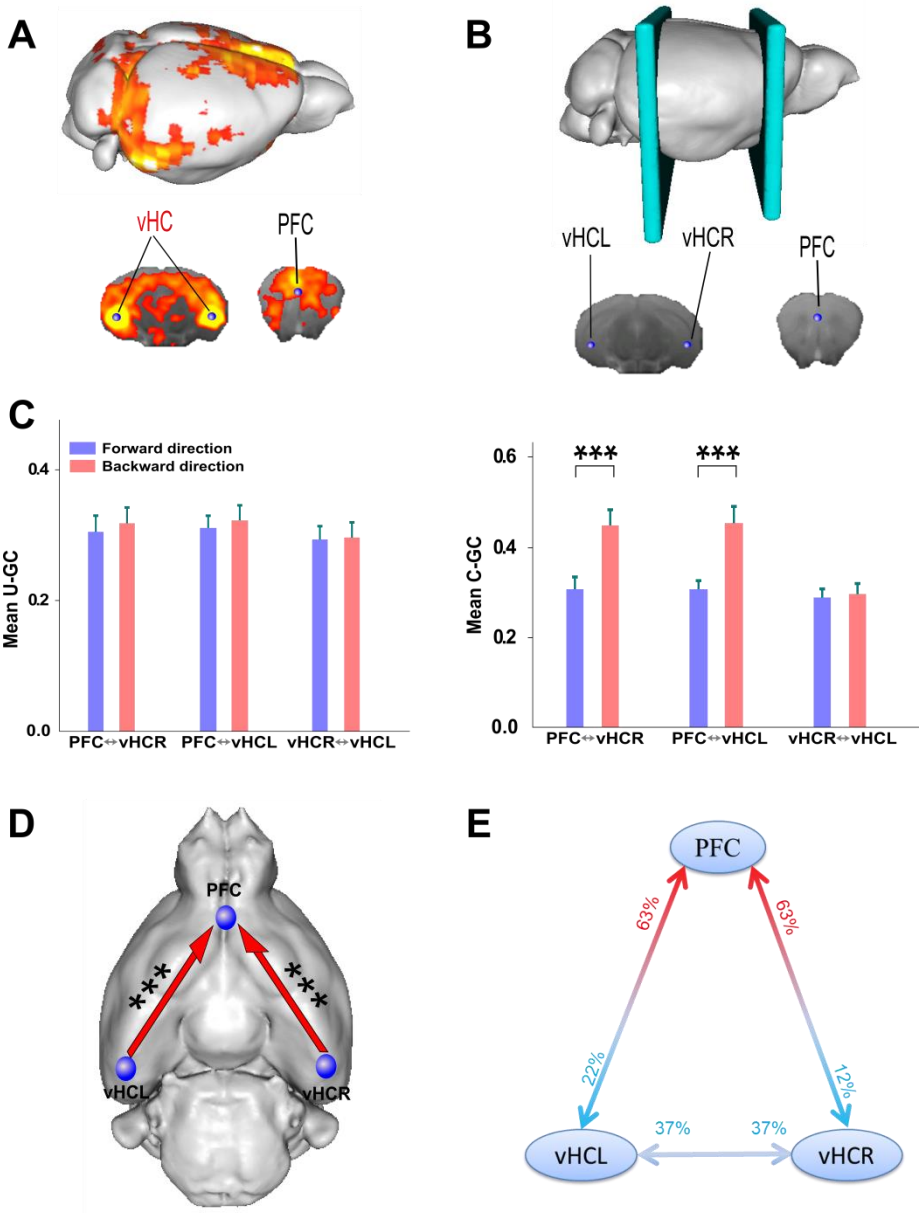

Figure 2.1

Figure 2.1: (A) Ventral hippocampus(vHC) and Prefrontal Cortex (PFC) Network with seed-voxel correlation maps(T>3, cc=0.001, N=41) for selected seeds(in red) with strong anterior-posterior connectivity; (B) vHC and PFC seed location(A partial location of 3d slices on the top); (C) Mean +/- SEM across 41 mice of GC(Right U-GC and left C-GC). Black stars and section signs denote statistical significance (paired t-test (***p<0.0001)); (D) Graphical illustration of the dominant directional functional connectivity inferred from C-GC analysis; (E) single subject level analysis by C-GC(Red : dominant directional percentage of significant number of subjects).

We first examined seed-based mapping and, consistent with previous rsfMRI findings (Schwarz et al. 2013; Sforazzini et al. 2014b) we found robust correlation between ventro hippocampal and prefrontal regions (Fig 2.1A,B). We thus defined a 3-node network made of left and right ventro-hippocampal regions, and a prefrontal (prelimbic) ROI and we then used Granger causation to map the direction of information flow within network.

We compared two measures characterized by distinct potential computational advantages: pairwise unconditional GC (U-GC) computes causation only examining the time series of two nodes and ignoring the other nodes, and as such it has the advantage that it is simple and data robust but on the other hand it is more prone to missing the detection of spurious causation due to the confounding effect of other neglected variables (see Methods). Conditional GC (C-GC), on the other hand, has the advantage that it can remove spurious causations due to the effect of the variable that is conditioned upon and so can add more information to the unconditional calculation, but its inherent complexity makes it more data-intensive and may have less statistical power in conditions where data are scarce. Which approach is better may depend on the experimental conditions. Given that the network we tested was made of 3 nodes, in computation of C-GC we conditioned GC between two nodes on the activity of the other node (we call this conditioning on a single variable 1C-GC, see Methods).

We found that pairwise U-GC did not highlight any dominant connectivity direction between any of the ROI pairs, (Fig. 2.1C) whereas pairwise C-GC revealed a robust dominant connectivity pattern between ventral hippocampal and prefrontal ROIs (***$p<0.0001$) along the direction of projecting ventro-subicular-prefrontal neurons, but not within left and right hippocampal areas. Thus, under the present conditions, C-GC was the marker of directed functional that – under the present experimental conditions - better matched the strong expectations set by anatomy. These findings highlight the ability of C-GC to unmask robust directional connectivity between rsfMRI node pairs. Based on this result subsequent analyses of 3-node networks were carried using C-GC only.

To assess inter-subject variability for GC-based directional connectivity readouts, single subject analysis was performed using a nonparametric surrogate test (Schreiber and Schmitz, 2000). Statistically significant ($p < 0.05$, FDR corrected) hippocampal-prefrontal directional connectivity was detected in 63% and 63% of the subjects for left and right hippocampal ROIs, respectively (Fig. 2.1E, 95% CI).

To probe network specificity of our findings, we repeated C-GC analysis employing different sets of ROIs within the hippocampal-prefrontal network. Specifically, we chose to probe sets of regions covering caudal ventro-hippocampal locations as well as rostral prefrontal regions (prelimbic) that are neuroanatomical components of this network, but that may be more prone to air-tissue susceptibility effects owing to their vicinity to ear canals and olfactory turbinates. The results for two representative sets of regions are reported in Fig 2.2. Seed-voxelwise

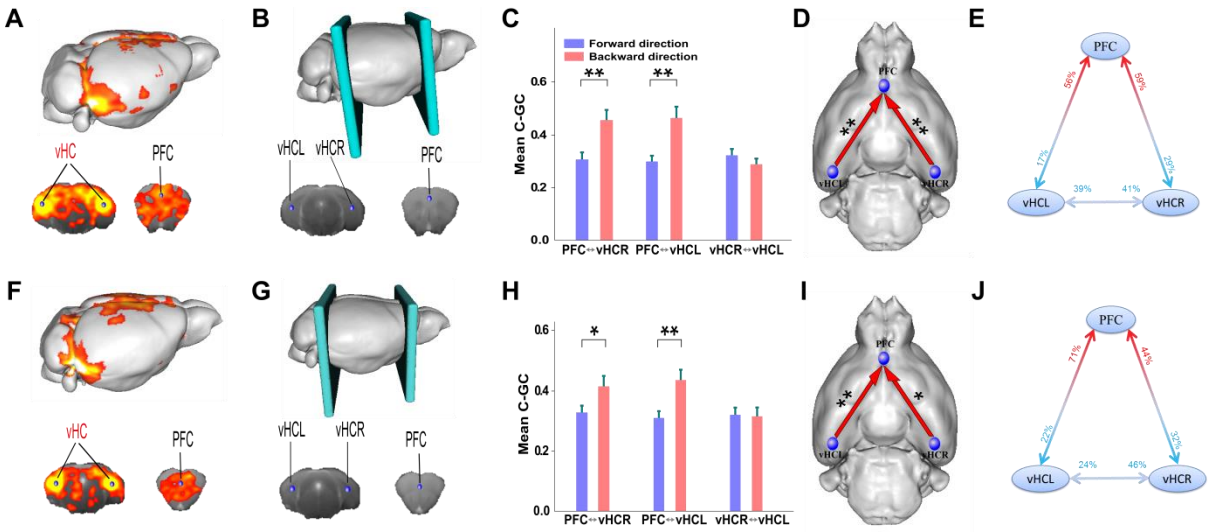

Figure 2.2

Figure 2.2: Represents two different sample sets of vHC-PFC network,((A)-(E) posterior vHC and dorsal PFC; (F)-(J) posterior vHC and anterior PFC; (A) & (F) seed-voxel correlation maps(T>3, cc=0.001, N=41) for selected seeds(in red) with strong anterior-posterior connectivity; (B) & (G) seed location including 3d slices; (C) & (H) Mean +/- SEM across 41 mice of C-GC. Black stars and section signs denote statistical significance (paired t-test (*p<0.05 & **p<0.001)); (D) & (I) Graphical illustration of the dominant directional functional connectivity inferred from C-GC analysis; (E) & (J) Single subject level analysis by C-GC(Red : dominant directional percentage of significant number of subjects).

correlation mapping revealed robust hippocampal-prefrontal rsfMRI connectivity patterns (Fig 2.2A,B and F,G). Consistent with our previous findings, GC causation was highly significant for all the three ROI pairs (Fig 2.2C, H, *p< 0.05 & **p< 0.001) and conditional (but not pairwise) GC revealed statistically-significant dominant ventral-hippocampal prefrontal connectivity for both the ROIs sets (Fig 2.2C,D and H,I). Single-subject analysis also produced evidence of dominant hippocampal-prefrontal connectivity in a large-proportion of subject for both ROI sets (Fig 2.2E,J), although the effect was smaller when

more distal brain slices were covered (56% and 59%, Fig 2E, 71% and 44% Fig 2J, respectively). Taken together, these findings highlight robust directional connectivity patterns within the hippocampal-prefrontal rsfMRI network along the direction of projecting ventro-hippocampal neurons, and support the use conditional GC to dissect dominant connectivity patterns in three-node ROIs sets.

Directional connectivity of insular-cingulate("salience") network

We next probed the presence of directional connectivity within the insular-prefrontal network, a set of regions previously described in the mouse to encompass the anterior insular cortex , dorsal and anterior cingulate cortex (Sforazzini et al. 2014b) that recapitulate general anatomical features of an analogous human rsfMRI network ("salience network") involved in the attribution of salience to environmental and behavioural stimuli (Seeley et al. 2007).

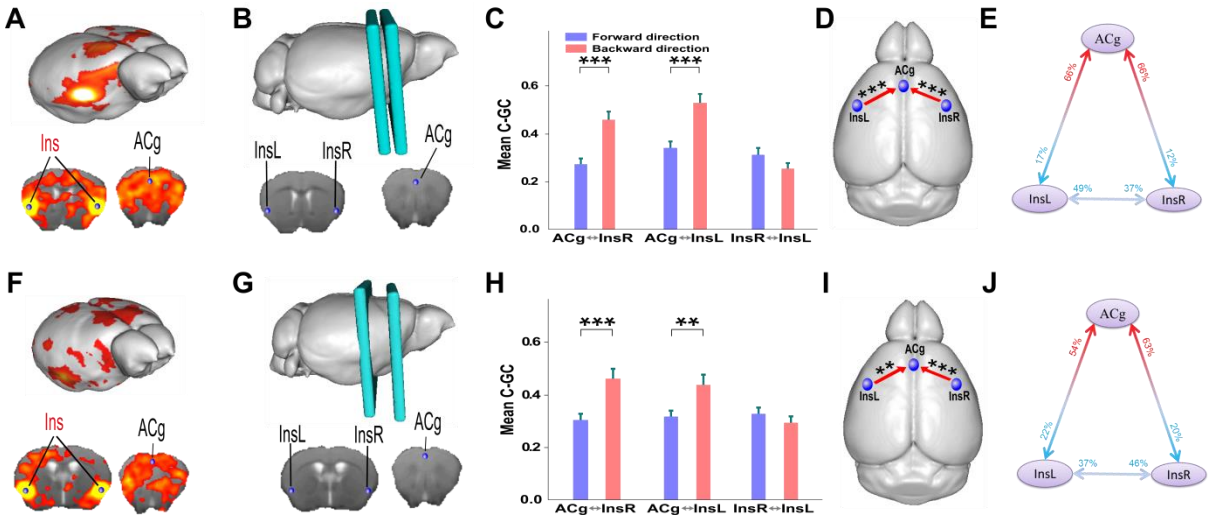

Figure 2.3

Figure 2.3: Represents two different sample sets of Salience network;(A)-(E) anterior Insular and PFC; (F)-(J) posterior Insular and dorsal PFC; (A) & (F) seed-voxel correlation maps(T>3, cc=0.001, N=41) for selected seeds(in red) with strong anterior-posterior connectivity;(B) & (G) seed location including 3d slices; (C) & (H) Mean +/- SEM across 41 mice of C-GC. Black stars and section signs denote statistical significance (paired t-test

(*p<0.05,**p<0.001 & ***p<0.0001));(D) & (I) graphical illustration of the dominant directional functional connectivity inferred from C-GC analysis; (E) & (J) Single subject level analysis by C-GC(Red : dominant directional percentage of significant number of subjects).

The underlying axonal connectivity of this network involves complex, reciprocal projections between cortical areas (Vertes 2004; Hoover and Vertes 2007; Zingg et al. 2014) which as such do not permit to predict a putative preferential direction of causation solely based on its structural architecture.

Voxelwise seed-mapping highlighted robust correlations between insular and dorso-prefrontal areas (Fig. 2.3A), replicating previous findings (Sforazzini et al. 2014a, 2014b). An effect associated to robust dominant insular-prefrontal connectivity observed in both left and right insular ROIs (Fig 2.3D, **p< 0.001 & ***p< 0.0001). No significant dominant inter-hemispheric connectivity was observed. In keeping with these findings, subject level analysis revealed dominant insular-prefrontal directional connectivity in 66% and 66% of the subjects (left and right insular cortex, respectively).

Conditional GC analysis employing a different set of ROIs covering more posterior insular locations confirmed the observed topological organization of this network (Fig 2.3F-J). Statistically significant directional connectivity between insular and anterior cingulate was observed both at the group level (Fig. 2.3H,I), and subject level in 54-63% of the subjects (Left and right insular ROI, respectively, Fig. 2.3J). These results highlight the presence of dominant antero-posterior functional connectivity patterns within the mouse insular-cingulate network reminiscent of directional features recently described for the human insular-cingulate (salience) network (Sridharan et al. 2008; Deshpande et al. 2011).

GC analysis of four-node rsfMRI networks

Directional connectivity mapping of the human DMN has typically entailed the use of four-node ROI sets permitting simultaneous probing of midline and latero-cortical antero-posterior seed locations (Jiao et al. 2011; Miao et al. 2011; Zhou et al. 2011; Di and Biswal 2014). To establish how to best compute directed connectivity with GC measures in four-node networks under the present experimental conditions, we integrated our previous hippocampal-frontal network ROI set (Fig. 2.1) with a fourth additional node (retrosplenial cortex) exhibiting significant connectivity with ventral hippocampal areas (Schwarz et al. 2013; Sforazzini et al. 2014b), and computed for each pair of nodes pairwise GC (Fig 4). As stated above, we used the hippocampal-prefrontal network to validate our approach because of its simple connectional configuration.

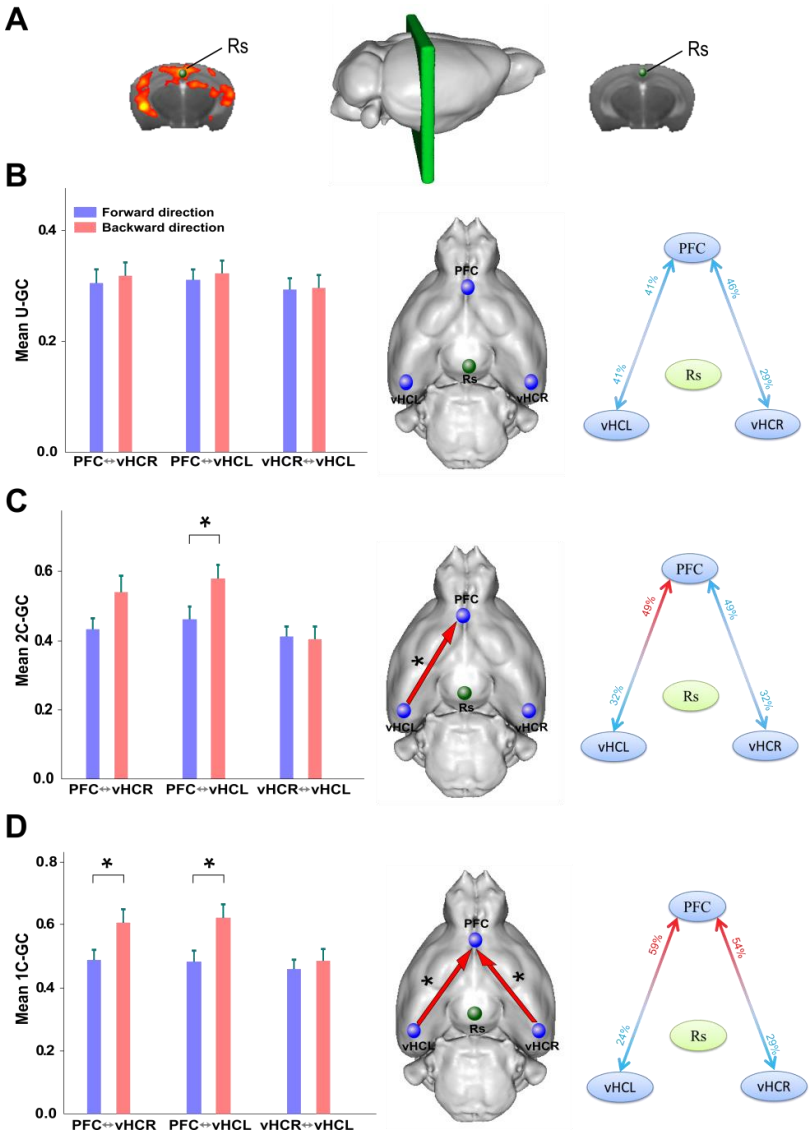

Figure 2.4

Figure 2.4: Represents validation of four nodes network by vHC-PFC network with adding Restrospenial(Rs) seed in Figure 1 network; (a) seed correlation maps in Rs slice(T>4, cc=0.0001, N=41) , location including 3d slice and position; (b) U-GC; (c) 2C-GC; (d) 1C-GC; ((b)-(d) right: Mean +/- SEM across 41 mice of GC; Black stars and section signs denote statistical significance (paired t-test (*p<0.05)), middle: Graphical illustration of the dominant directional functional connectivity inferred from GC analysis and left: Single subject level analysis by GC(Red : dominant directional percentage of significant number of subjects)).

We examined the robustness in retrieving this expected directional connectivity with three possible ways to compute GC: U-GC where causation between two nodes is computed only using those two nodes and ignoring the others; 1C-GC where causation between two nodes is computed by conditioning on one of the other two nodes at a time and then averaging the so obtained values across the two different choices of conditioning nodes; and 2C-GC where causation between two nodes is computed by conditioning on the other two nodes. For each of these computational strategies and pair of nodes, we did observe robust causation (Fig. 2.4, *$p<0.05$). Among these measures, 1C-GC, but not pairwise U-GC and 2C-GC revealed statistically significant bilateral directional connectivity between ventro-hippocampal and prefrontal areas consistent with what observed using three-node ROI sets (Fig 4B, C and D). This results shows that also in this case, the 1C-GC measure gives an optimal trade-off between the need to discount confounders and the need to keep the model as simple as possible to increase data robustness and statistical power. Therefore, in all subsequent analyses of 4-node networks we used 1C-GC as a measure of directed causation among nodes. Although the result obtained with 1C-GC were fully consistent with those found in the corresponding 3-node network (Fig. 2.1), the effect was weaker when using 4-node ROI sets (*$p<0.05$), suggesting that under our experimental conditions, statistical power is strongly node-number limited.

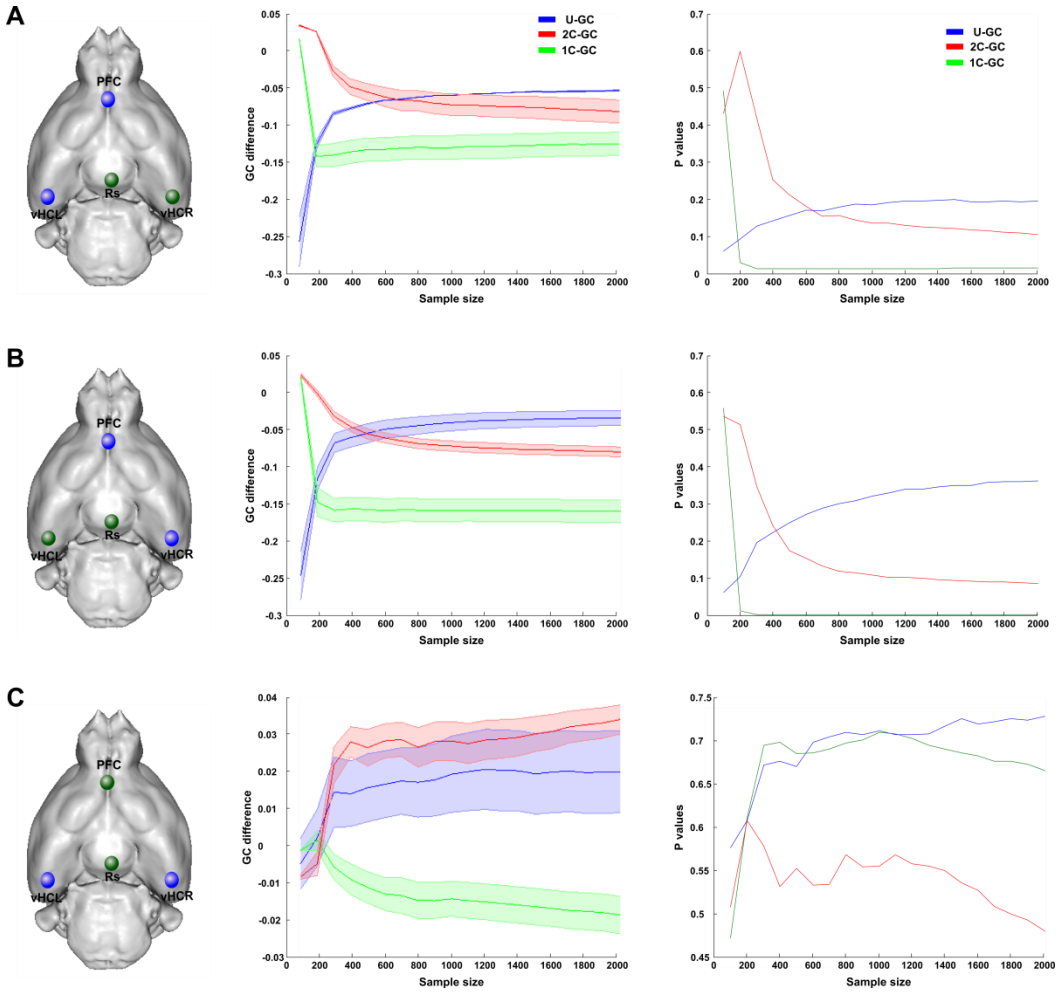

Figure 2.5

Figure 2.5: Simulations to investigate the most efficient calculation of GC on this data; (A), prefrontal cortex and left ventral Hippocampus, (B), prefrontal cortex and Right ventral Hippocampus, (C), right ventral Hippocampus and left ventral Hippocampus; [Left panels: location of the ROIs where blue cube represents paired ROIs and green cube represents the confounders to compute GC, middle panels: mean +/- SEM GC difference across subject and right panels: p-values obtained by paired t test].

To examine the robustness of the different GC measures (U-GC,1C-GC,2C-GC) to the sample size, we generated simulated time series from the full VAR model selected for each subject (see Methods). Given that the models fit the original data, the GC values obtained in the limit of a big data size will match the ones obtained for these data. The degree to which

GC values estimated for smaller data sizes differ from that limit will indicate how robust the estimates are. In particular, we are interested in examining the changes that occur for a sample size equal the actual sample size of the fMRI data, i.e., 300 data points. In Figure 2.5 we can see, for the PFC-RS-vHC network, how GC differences and p-values (paired t test across subjects) change with the sample size. For the GC differences that were found significant when using 1C-GC on the original data, that is, from PFC to vHCL and from PFC to vHCR (Figure 2.5A, B, respectively), we see that 1C-GC is the most robust GC measure, with an almost invariant GC difference value as a function of sample size down to sample sizes smaller than 300 data points. Similarly, p-values remain robustly significant for 1C-GC for our experimental data size. In the case of GC differences from vHCL to vHCR, they remain small and insignificant in the whole range of sample sizes examined, in agreement with the values obtained for the original data. These results support that 1C-GC is the most suitable GC measure given the sample size of our recordings and the dynamics of the fMRI time series.

Directional connectivity of the mouse "default mode network"

ICA revealed the presence of significant rsfMRI correlation between prefrontal and orbitofrontal regions, cingulate and retrosplenial cortex, as well as temporal cortical areas (Fig 2.6A, Z >1), thus recapitulating rodent patterns of spontaneous correlated activity that have been postulated to represent a rodent homologue of the human DMN (Lu et al. 2012; Sforazzini et al. 2014b) . Analogous rsfMRI network features were obtained using seed-based correlation mapping (Fig. 2.6B).

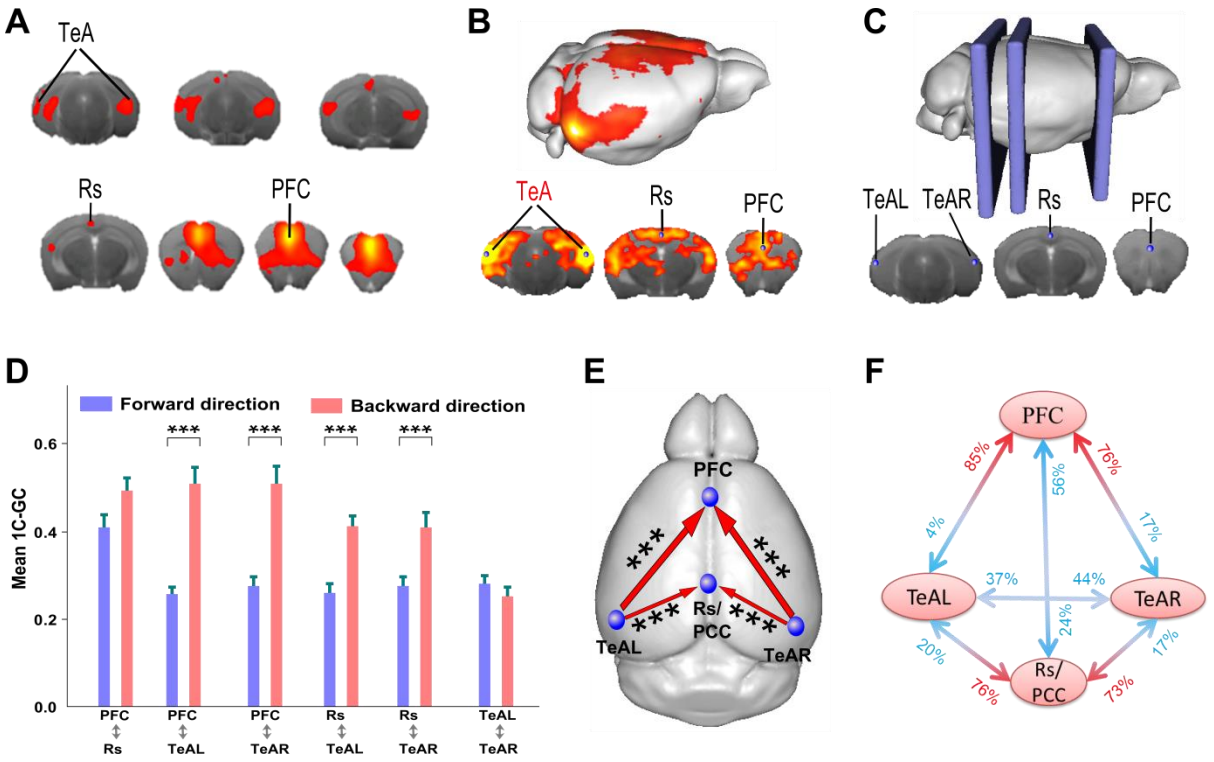

Figure 2.6

Figure 2.6: Default mode network(DMN); (A) independent component analysis(ICA) (Z >1); (B) Temporal Association cortices (TeAL & TeAR,), Restrospenial(Rs) and Prefrontal Cortex (PFC) seed-voxel correlation maps(T>4, cc=0.0001, N=41) for selected seeds(in red) with strong connectivity, (C) seed location including partial position of 3d slices; (D) Mean +/- SEM across 41 mice of 1C-GC. Black stars and section signs denote statistical significance (paired t-test (***p<0.0001));(E) Graphical illustration of the dominant directional functional connectivity inferred from 1C-GC analysis; (F) Single subject level analysis by 1C-GC(Red : dominant directional percentage of significant number of subjects).

GC analysis of key DMN nodes (i.e. temporal association, retrosplenial and prelimbic cortices) revealed a symmetric pattern of robust directional connectivity between temporal association cortex and retrosplenial and prefrontal areas(Fig. 2.6D and E, ***p<0.0001). No significant directional inter-hemispheric connectivity was observed between homotopic temporal cortical regions. In keeping with these findings, subject level analysis revealed

analogous dominant directional connectivity in the majority of the subjects examined (85-76%, temporal association to prefrontal cortex; 76-73% temporal association to retrosplenial, Fig. 2.6F). Similar patterns of directional connectivity could be obtained using separate 4-node ROI sets covering different locations. The results of GC in a representative set covering more anterior temporal cortex locations, and more posterior retrosplenial cortex placement is depicted in Figure 2.7. GC analysis of this ROI set revealed similarly robust dominant connectivity signatures (Fig. 2.7D and E), together with a higher incidence of individual subjects showing significant directional connectivity patterns (68-85%, temporal association to prefrontal cortex; 82-82% temporal association to retrosplenial, Fig. 2.7F). These results highlight the presence of robust directional functional connectivity between temporal associative cortical regions and prefrontal regions, together with a "sink effect" of retrosplenial cortex with respect of temporal cortical areas.

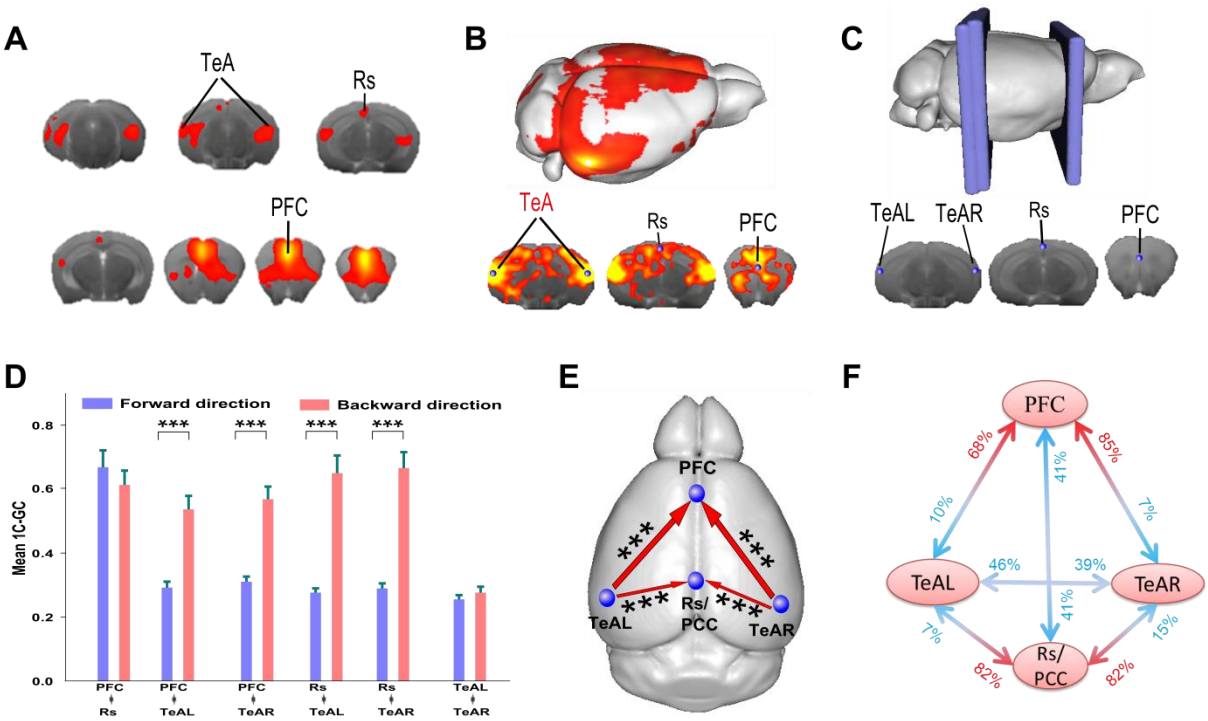

Figure 2.7

Figure 2.7: Another circuit of default mode network(DMN); (A) independent component analysis(ICA) (Z >1); (B) Temporal Association cortices (TeAL & TeAR,), Restrospenial(Rs) and Prefrontal Cortex (PFC) seed-voxel correlation maps(T>4, cc=0.0001, N=41) for selected seeds(in red) with strong connectivity; (C) seed location including partial position of 3d slices; (D) Mean +/- SEM across 41 mice of 1C-GC. Black stars and section signs denote statistical significance (paired t-test (***p<0.0001));(E) Graphical illustration of the dominant directional functional connectivity inferred from 1C-GC analysis; (F) Single subject level analysis by 1C-GC(Red : dominant directional percentage of significant number of subjects).

More broadly our results highlight the possibility of applying GC-based methods to infer robust directional connectivity patterns in the living mouse brain. The robustness and specificity of our findings was corroborated by the results of two additional control analyses. First, it has been reported (Quiroga et al., 2000) that interactions or causality measures between time series tend to be biased in the direction from low to high frequencies (see e.g. Quiroga et al. 2000, Fig. 2). We therefore computed the spectral properties (spectral power density and center frequency) of the fMRI time course within all ROIs examined within our networks (Fig. 2.8). We found that in all networks the node receiving causation (PFC or Rs had the slowest (**p < 0.001 &***p < 0.0001) center frequency. (Fig. 2.8A-C). Since our experimental results report positive strongest causality in the direction from high to low frequencies, these considerations suggest that the experimental findings do not trivially reflect frequency differences in the signals.

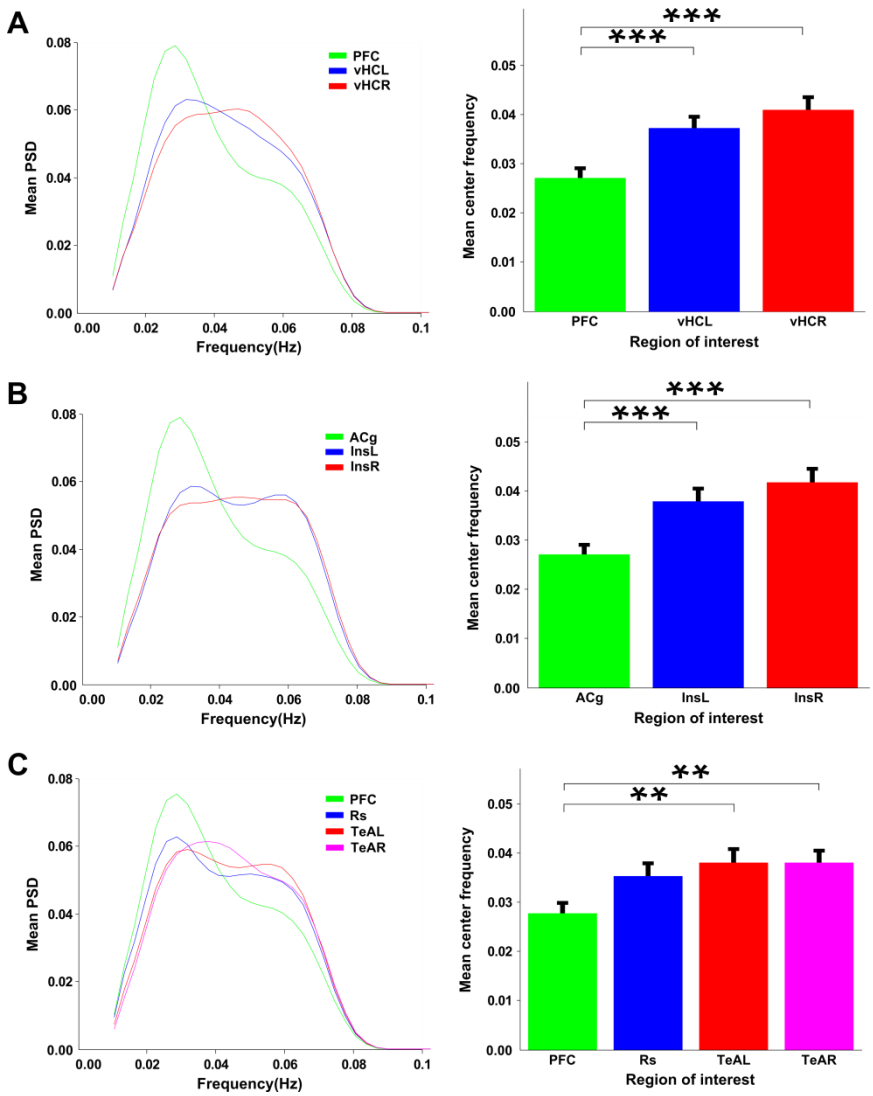

Figure 2.8

Figure 2.8: Subject average Power spectral density (PSD) & center frequency(CF) of three different networks from preprocessed data; (A) vHC-PFC network of figure 2(top sample); (B) Salience Network of figure 3(top sample) (C) DMN of figure 5; ((A)-(C) right: average PSD between 0.01 to .08 Hz; left: average center frequency (black star: paired t-test between ROIs'(**p<0.005 & ***p<0.0005))

Second, to account for potential bias induced by surface coil-induced regional variation in temporal signal to noise ratio (tSNR), we repeated GC analyses on rsfMRI timeseries corrupted with random pink noise such to achieve homogenous tSNR levels equalling values observed in deep subcortical areas (≈ 25). The results of this analysis (Fig. 2.9A, B,C and D)

confirmed original directional connectivity signatures of the network (*p < 0.05, ***p < 0.0001 , FDR corrected) thus ruling out a significant contribution of coil-related bias on the identified dominant connectivity patterns.

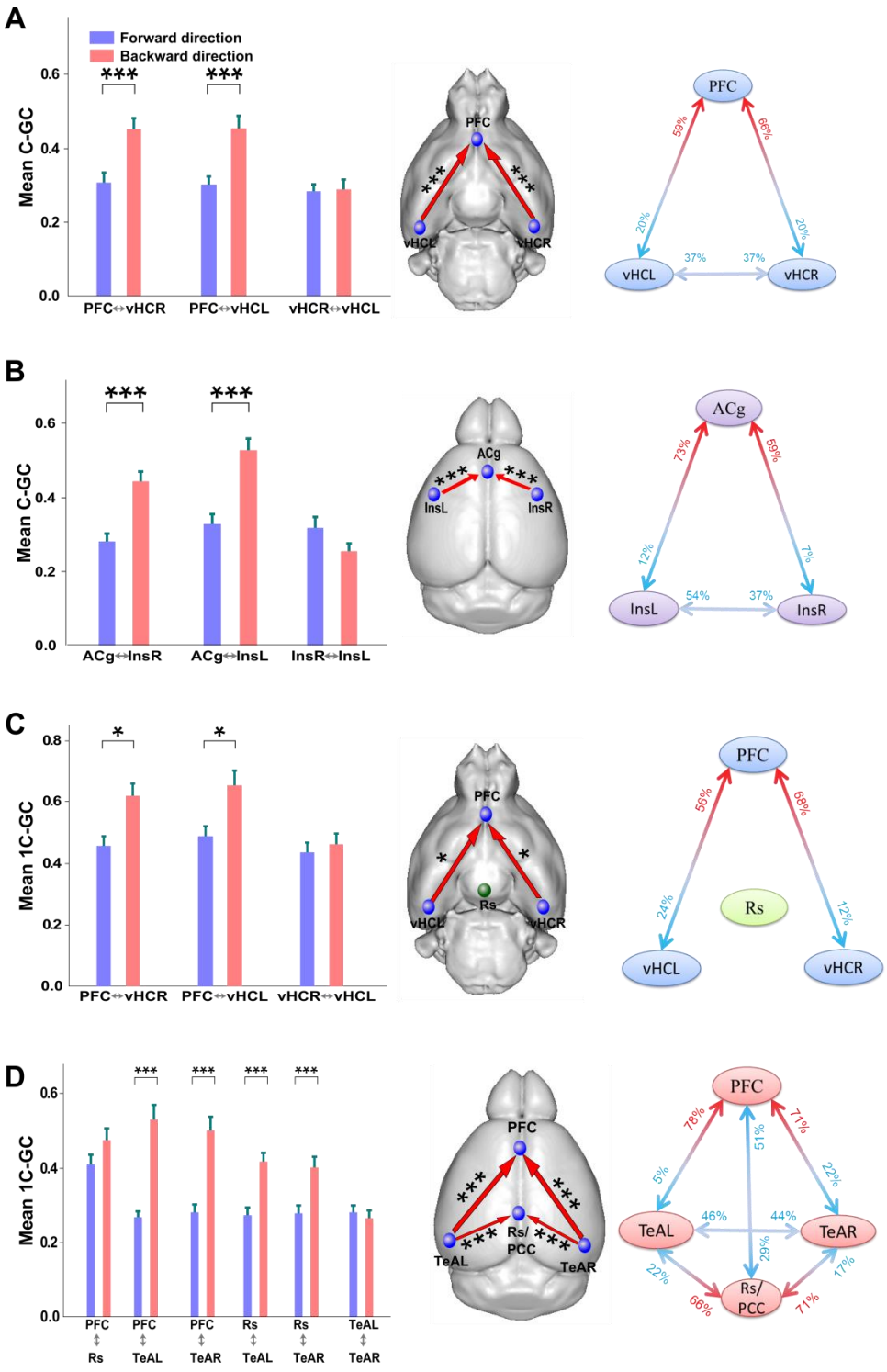

Figure 2.9

Figure 2.9: GC analysis with added pink noise over different networks; (A) vHC-PFC network of figure 1; (B) SN of figure 3;(C) vHC-Rs-PFC network of figure 4; (D) DMN of figure 5; ((A)-(D) right: Mean +/- SEM across 41 mice of GC, black stars and section signs denote statistical significance (paired t-test (*$p<0.05$ & ***$p<0.0001$)), middle: Graphical illustration of the dominant directional functional connectivity inferred from GC analysis and left: Single subject level analysis by GC(Red : dominant directional percentage of significant number of subjects)).

An autism-related mutation alters directional connectivity in the mouse SN & DMN

Human imaging studies have consistently revealed altered rsfMRI connectivity across brain regions of autism spectrum disorder (ASD) patients (Anagnostou and Taylor 2011). However, fundamental questions as to the origin and interpretation of these findings remain unanswered. For one, the neurophysiological underpinnings of these connectional derangements are largely unknown, and a causal etiopathological contribution of specific genetic variants to impaired connectivity in ASD remains to be established.

Mouse models harboring mutations with robust ASD-association can provide novel insights into the pathogenesis of such aberrant connectivity. The use of rsfMRI in mouse lines characterised by high confidence ASD-associated mutation can be used to establish causal relationships between specific genetic aetiologies and aberrant macroscale connectivity.

To assess the potential of using directional connectivity mapping in models displaying connectivity aberrations, we used GC mapping of rsfMRI in contactin-associated protein like-2 (Cntnap2) “knock-out” mice (Peñagarikano et al. 2011). Human homozygous carriers of aCntnap2 bnormal alleles exhibit reduced long-range rsfMRI connectivity and aberrant white matter microstructure (Scott-Van Zeeland et al. 2010; Clemm von Hohenberg et al. 2013). Cntnap2-/- mice show behavioural phenotypes relevant to ASDs and impaired local cortical

synchrony (Peñagarikano et al. 2011). Moreover, human homozygous carriers of Cntnap2 abnormal alleles exhibit reduced long-range rsfMRI connectivity and aberrant white matter microstructure (Scott-Van Zeeland et al. 2010; Clemm von Hohenberg et al. 2013) thus hinting at the possible presence of functional connectivity alterations in this strain.

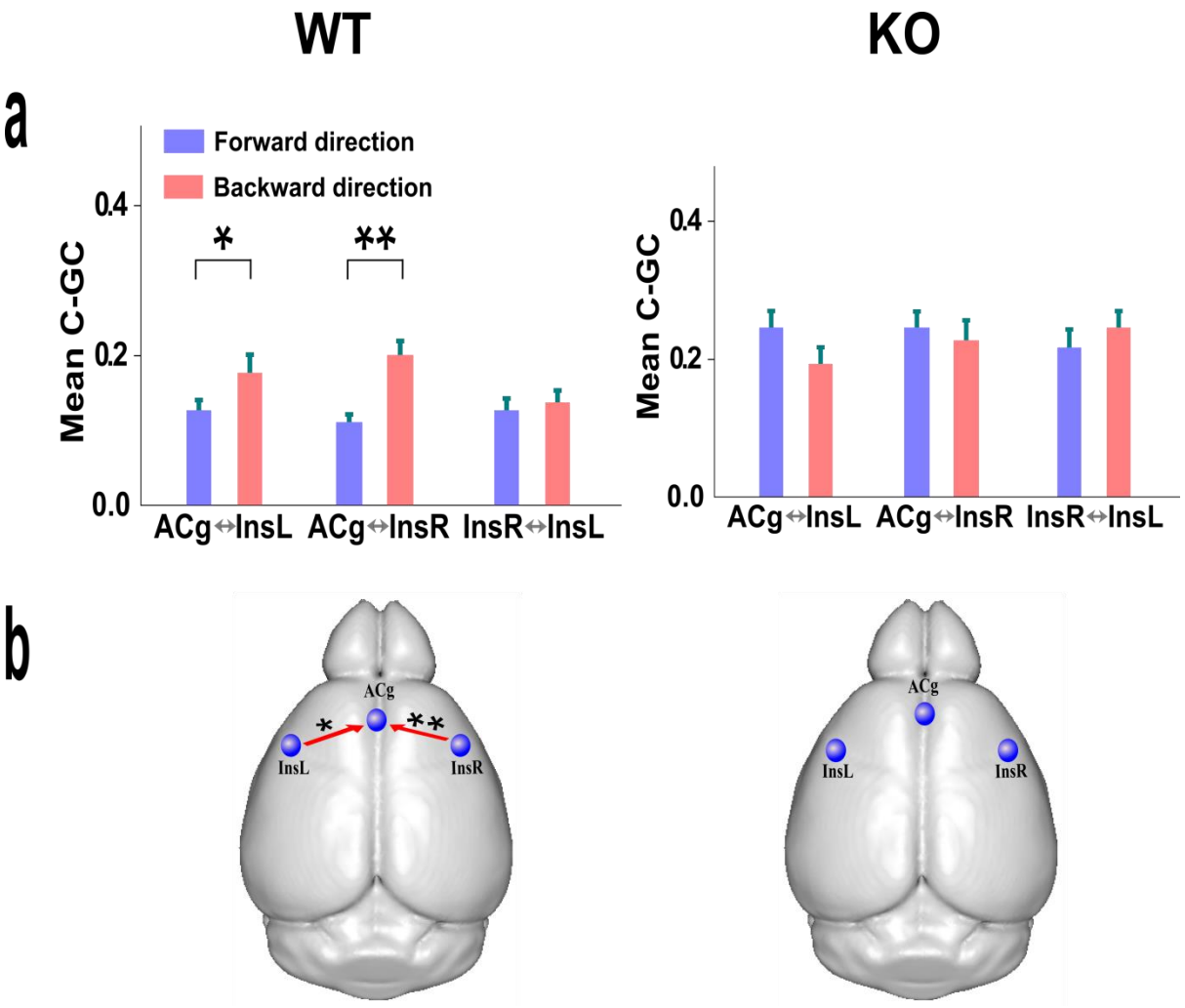

Figure 2.10

Figure 2.10: Comparison of C-GC results in the salience network obtained with either a sample of 14 control subjects (left panels) or a sample of 13 transgenic subjects (right panels). The same set of ROIs was used in both conditions; (a), mean +/- SEM of C-GC for all ROI pairs reveal significant directional effects (*p<0.05 & **p<0.001 asymmetry in GC, paired t-test). (b), graphical illustration of the dominant directional functional connectivity inferred from GC analysis.

Consistent with our previous findings GC analysis revealed significant directional connectivity in the salience network of control mice (wild type – WT). Interestingly, no dominant connectivity direction was observed in Cntnap2-/- mutants (KO)(Fig 2.10). Similarly, a pattern of robust directional connectivity was observed in the DMN both at single subject and population level in control (WT) mice. However, no significant dominant directional flow of information was found in Cntnap2 mutants between lateral temporal and prefrontal areas, and intriguingly, in this cohort the causal influence between temporal association and retrosplenial cortices was reversed(Fig 2.11). The presence of a no or reversed causal inference in mutants could be related to the presence of altered cortical layering observed in these mice, a finding that may give rise to abnormal macroscale oscillatory dynamics (Peñagarikano et al. 2011). This dataset is also important as it represent a confirmation of the reproducibility of the directional patterns observed in a different experimental cohort.

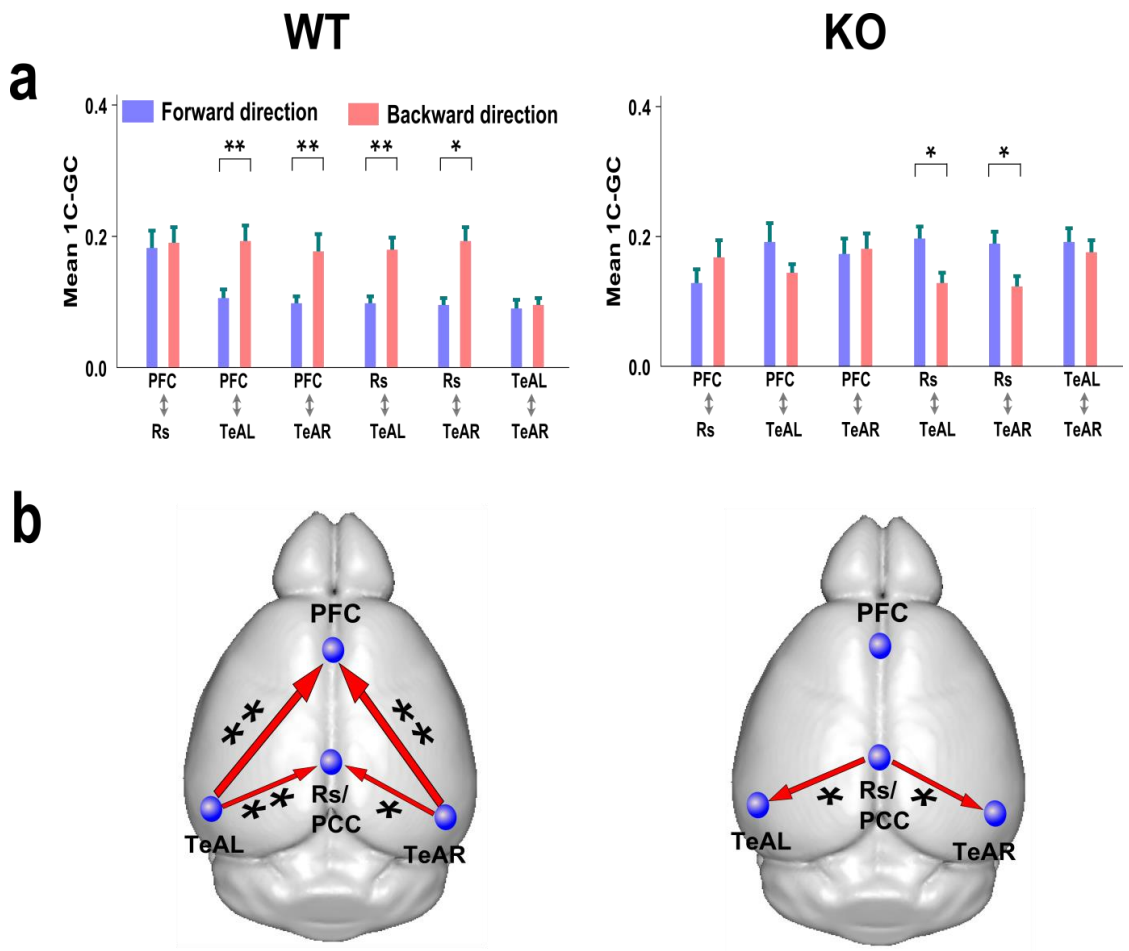

Figure 2.11

Figure 2.11: Comparison of 1C-GC results in the default mode network obtained with either a sample of 14 control subjects (left panels) or a sample of 13 transgenic subjects (right panels). The same set of ROIs was used in both conditions; (a), mean +/- SEM of C-GC for all ROI pairs reveal significant directional effects (*p<0.05 & **p<0.001 asymmetry in GC, paired t-test). (b), graphical illustration of the dominant directional functional connectivity inferred from GC analysis.

Chapter 3 **: Discussion**

A major goal of current brain research is to understand and describe how information dynamically propagates and link different brain regions, generating maps of brain functional connectivity. Prevalent functional connectivity approaches, such as the use of spontaneous BOLD rsfMRI signal fluctuations, have been successfully applied to describe the large-scale functional organization of the human brain. The extension of this approach to laboratory animals such as the mouse has been recently proposed, highlighting encouraging cross-species neuroanatomical correspondences between rsfMRI networks identified (Sforazzini et al. 2014b). However, rsfMRI-based connectivity typically relies on measurements intrinsically insensitive to the direction of information flow among affected regions, thus limiting the possibility of effectively describing their interaction and communication. By using GC we show that distributed mouse brain rsfMRI networks, such as the DMN, are characterised by robust directional connectivity patterns exhibiting convergent information flow towards integrative mouse brain regions, thus shedding new light on the brain's functional organization.

Similar attempts to map the direction of information flow within human brain rsfMRI systems have been recently described using different computational approaches, including GC(Deshpande et al. 2011; Uddin et al. 2011; Zhou et al. 2011), Bayesian networks (Wu et

al. 2011), partial directed coherence and dynamic causal modelling (Li et al. 2012; Razi et al. 2014; Crone et al. 2015). Despite large heterogeneity in the methodological approaches employed, conserved directional features within distributed human rsfMRI systems are emerging. For example, directional connectivity patterns linking lateral (e.g. temporal/parietal associative areas) and midline (e.g. prefrontal and posterior cingulate/retrosplenial cortex) nodes of the human DMN have been described by several independent investigators (Jiao et al. 2011; Miao et al. 2011; Silfverhuth et al. 2011; Zhou et al. 2011; Di and Biswal 2014; Razi et al. 2014; Crone et al. 2015). Preliminary evidence for a casual influence of anterior insular regions on anterior cingulate and prefrontal areas has also been recently described (Sridharan et al. 2008; Deshpande et al. 2011; Chen et al. 2015). These initial results suggest the presence conserved directional signatures defining a hierarchical relationship between brain regions also in task-free "resting-state" conditions.

The rsfMRI networks probed in the present work recapitulate prominent neuroanatomical features of known human rsfMRI systems that justify a tentative cross-species comparison of the directional pattern identified. For example, the insular-cingulate network mapped in this work and in previous studies (Sforazzini et al. 2014a, 2014b) presents significant involvement of anterior cingulate and dorsal prelimbic cortices, two neuroanatomical regions that display cyto-architectural properties of human brain Brodmann area 24 (Vogt and Paxinos 2014), the key prefrontal node of the human salience network (Seeley et al. 2007). Although at present it is unclear whether the mouse homologue of this network exerts a similar role in salience attribution, and notwithstanding possible topological differences in rodent and primate insular organization, the observation of analogous insular-prefrontal directional connectivity patterns in mice and human is suggestive of a possible evolutionary relationship between the two rsfMRI systems. In the case of the mouse DMN, despite the presence of apparent neuroanatomical similarities between rodent and human DMN

organization (Lu et al. 2012; Sforazzini et al. 2014b), cross-species comparison between directional connectivity findings are complicated by the lack of mouse cyto-architectural homologues for human DMN nodes in which directional connectivity has been probed (e.g. inferior parietal lobule, or lateral temporal cortex), and by the unknown (and at present largely speculative) evolutionary trajectory of this network in the mammal brain. Despite these limitations, and the great heterogeneity in the approaches so far employed for human effective connectivity mapping, the observation of dominant connectivity between lateral temporal regions and retrosplenial cortex (precuneus in humans) reproduces a directional feature consistently observed by several directional investigations of the human DMN (Jiao et al. 2011; Miao et al. 2011; Zhou et al. 2011; Di and Biswal 2014; Razi et al. 2014; Wu et al. 2014; Crone et al. 2015). Evidence for a directional influence of lateral temporal regions on medial prefrontal areas has similarly been reported by a number of investigators (Deshpande et al. 2011; Jiao et al. 2011; Di and Biswal 2014; Razi et al. 2014; Wu et al. 2014), although some reports have described opposite connectivity patterns (Zhou et al. 2011). Other directional features, such as the presence (or lack thereof) of directional connectivity between prefrontal and precuneus/retrosplenial areas have not been consistently replicated (Di and Biswal 2014; Razi et al. 2014; Crone et al. 2015). Collectively, some degree of convergence exists in the directional patterns of rsfMRI connectivity between temporal cortical areas and midline DMN structures of the human and mouse brain, supporting the hypothesis of a conserved topological organization of these networks across species. Independent of the evolutionary relationship between these systems, the presence of intrinsic directional connectivity between antero-lateral insular and posterolateral temporal sub networks involved in large-scale sensory integration (Zingg et al. 2014) and medial prefrontal area involved in higher cognitive functions is consistent with hierarchical models of cortical function (Badre 2008; Holroyd and McClure 2014).

The identification of robust directional connectivity between subicular regions and prelimbic areas is of interest, because the dominant direction identified follows the putative unidirectional axonal connectivity between these two regions (Hurley et al. 1991; Takagishi and Chiba 1991; Vertes 2004). This observation suggests that GC-based directional connectivity mapping of rsfMRI networks may reveal causal relationship between neural systems that are constrained by underlying anatomical connectivity, in the same way analogous information theory approaches are utilized to established causal relationship using integrative electrophysiological readouts (e.g. local field potentials – LFP (Kamiński et al. 2001). However, further research employing interventional approaches aimed at modulating both neuronal activity (e.g. by inhibiting subicular neurons) and underlying connectional projection (e.g. via lesions or altered connectional wiring) are required to substantiate this link and disambiguate the neural drivers and connectional foundations of the directional effects mapped. It should also be emphasized that directional connectivity as inferred from neuronal signals is highly dynamic and strongly affected by behavioural and brain states (Adhikari et al. 2010; Brockmann et al. 2011), and as such may not directly translate into analogous rsfMRI directional patterns. In this respect, the implementation of GC and rsfMRI mapping in the mouse represent a major step forward toward a better comprehension of the neural bases of these directional signals, owing to the large repertoire of interventional approaches and genetic models that can be readily implemented to validate or disprove some of the assumptions underlying directional mapping via statistical inferences. Our subject level analysis demonstrate the possibility of detecting significant directional connectivity in individual subjects, although the lack of significant effects in all the imaged subjects suggest that cross-sectional designs could be more appropriate than longitudinal studies to probe directional connectivity in this species.

Importantly, we were able to confirm our directional connectivity signatures in an independent cohort of animals, as part of a study aimed at elucidating the presence of directional alteration in a transgenic mouse model of high translational relevance for autism research(Peñagarikano et al. 2011). The replicability of our directional findings in a separate cohort of mice is an important confirmation of the presence of region-specific intrinisic causal relationship between rsfMRI fluctuations originating in functionally-connected brain districts. The presence of altered directional connectivity in mice exhibiting autism related alterations leads us to speculate that some of the altered behavioural phenotypes (and possibly symptoms in patients) associated to this disorder may reflect altered or inefficient integrative function in high order cognitive systems. Further investigations into the origin and determinants of these connectional signatures are required to understand their neurobiological significance.

The fact that our experiments were performed under light anesthesia raises the question as to the whether the directional connectivity identified reflects the functional architecture of the mouse brain under conscious quite wakefulness (e.g. the resting-state). The challenges in implementing motion-sensitive readout like rsfMRI in awake/restrained mice prevent a straightforward answer to this experimental question. However, the anesthetic regimen employed in this study preserves cerebral blood flow autoregulation (Gozzi et al. 2007), cortical electrical responsiveness (Orth et al. 2006) , and has been show to lead to the identification of networks remarkably similar to those seen in conscious (and lightly anesthetised) rats and primates (Vincent et al. 2007; Hutchison et al. 2010; Lu et al. 2012; Schwarz et al. 2013). Importantly, we recently demonstrated excellent spatial correspondence between rsfMRI signals obtained during light halothane anaesthesia and electrophysiological coherence signals in freely-behaving mutant mice, suggesting that the anaesthetic protocol preserves fundamental neural signatures underlying intrinsic rsfMRI connectivity profiles

(Zhan et al. 2014). The empirical correspondences between directional connectivity patterns identified in the present work and analogous directional signatures in human rsfMRI networks are encouraging and argue against a substantial confounding role of anesthesia. The implementation of rsfMRI in awake habituated mice (e.g. under head-fixed conditions) may help disambiguate the effect of anesthesia. The use of alternative anaesthethic protocols leading to the identification of analogous networks (e.g. medetomidine,(Shah et al. 2015)) may also help identify the presence of anaesthesia-specific directional patters. More broadly, the parallel implementation of multisite electrophysiological coherence measurements (e.g. LFP) between the nodes probed in our study under similar anesthesia conditions and in behaving mice using wireless implants (Zhan et al. 2014) could in the meantime shed light on the neural origin of the robust directional signatures observed and to assess their relationship with brain states.

The mathematical method that we chose here to map directed connectivity is based on Granger Causality. There are many possible ways to estimate the direction and strength of connectivity from simultaneous time series of brain recordings, and the relative strengths and weaknesses of each method are under serious debate (Patel et al. 2006; David 2011; Friston 2011; Roebroeck et al. 2011a, 2011b, 2011c; Smith et al. 2011; Friston et al. 2014a; Liu et al. 2015). Some techniques, such as Dynamical Causal Modelling (DCM), estimate the direction of connections with a model based approach that makes strong assumptions about the underlying neural circuitry and about the coupling between neural activity and hemodynamics. The advantage of model based approaches is that they provide an explicit estimate of the circuit diagram of the considered neural network that takes into account possible difference in the "state" of each node of the network (due for example to differences in the balance between excitation and inhibition across nodes). The disadvantage of these model-based approaches is that they provide a potentially misleading picture of the circuit's

connectivity if the assumptions of the model are wrong. Given that relatively little is yet known about the neural properties of the neural circuits that we investigated and about neurovascular coupling in mice, we preferred here to take a safer approach using a techniques such as Granger Causality that does not make assumptions about neural and vascular mechanisms. However, and despite the relative generality of its assumptions, also the application of Granger causality presents elements of risk and of arbitrariness. In particular, the best way to maximize the sensitivity of Granger Causality calculations to asymmetries in the direction of communication depends on the nature of the data. We illustrated this point by investigating how the estimate of directional connectivity depends on the number of nodes we condition upon. The specific advantage of our work was that we used a double procedure to investigate the optimal number of conditioning nodes to detect asymmetries in Granger Causation. On the one hand, we produced simulate data with statistics close to the one of the real data and we investigated which conditioning method is more robust, finding unequivocally that conditioning on one node was the most robust procedure in this case. We then corroborated this finding by testing the different conditioning methods on a cortical network that has purely one-directional connections between two brain sites. In such condition, there is a clear plausible expectation of what the leading direction of causation should be. We found that also this validation confirmed that conditioning on one node was the most robust procedure in this case. Although testing algorithms of connectivity with simulations has been done before successfully (Honey et al. 2007; Smith et al. 2011; Deshpande and Hu 2012; Wen et al. 2013), the combination of testing with simulations and with plausible pieces of anatomical circuitry has not been done before to our knowledge. We suggest that such combined comparisons will be useful to contribute to perfection methods to estimate functional and effective connectivity for each dataset, and will ultimately contribute

to a better understanding of the functional and effective circuitry of the cerebral cortex in humans and animals.

In summary, we demonstrate robust directional connectivity patterns in distributed rsfMRI networks of the mouse brain, including converging dominant connectivity between lateral cortical areas and medial prefrontal and cingulate regions, replicating topological features of known human rsfMRI networks, and consistent with a higher integrative function subserved by these areas. Our work provides a first description of directional topology of mouse intrinsic connectivity networks, and sheds new light on the intrinsic functional organization of the mouse brain, thus complementing ongoing research in the macroscale functional architecture of this species.

Appendix: Control analysis on Granger Causality estimation from fMRI data

This chapter reports some control analyses that we did to corroborate the main analyses of Granger Causality directionality from fMRI data that were presented in Chapter 2.

Effect of deconvolution

As mentioned earlier in Chapter 2, previous studies have proposed that when estimating Granger Causality from fMRI data it is useful to deconvolve the fMRI data with a canonical hemodynamic response function, so that we operate on signals that have time scale closer to those of neural activity and so we may more easily capture the neural interactions happening at relatively fast time scales (Wu et al. 2013a). The canonical deconvolution approach (Wu et al. 2013a) presents several variants depending on how many of its derivatives are used. Here we tested the effect of using different variants on this method on the default mode network that we used as a test bed for fine-tuning our methods (see Chapter 2).

Most robust and consistent results for one-node conditional Granger Causality (1C-GC)were observed by applying 'canonical + time derivative' model option (Fig. A.1).We thus followed this option for all networks reported in this Thesis.

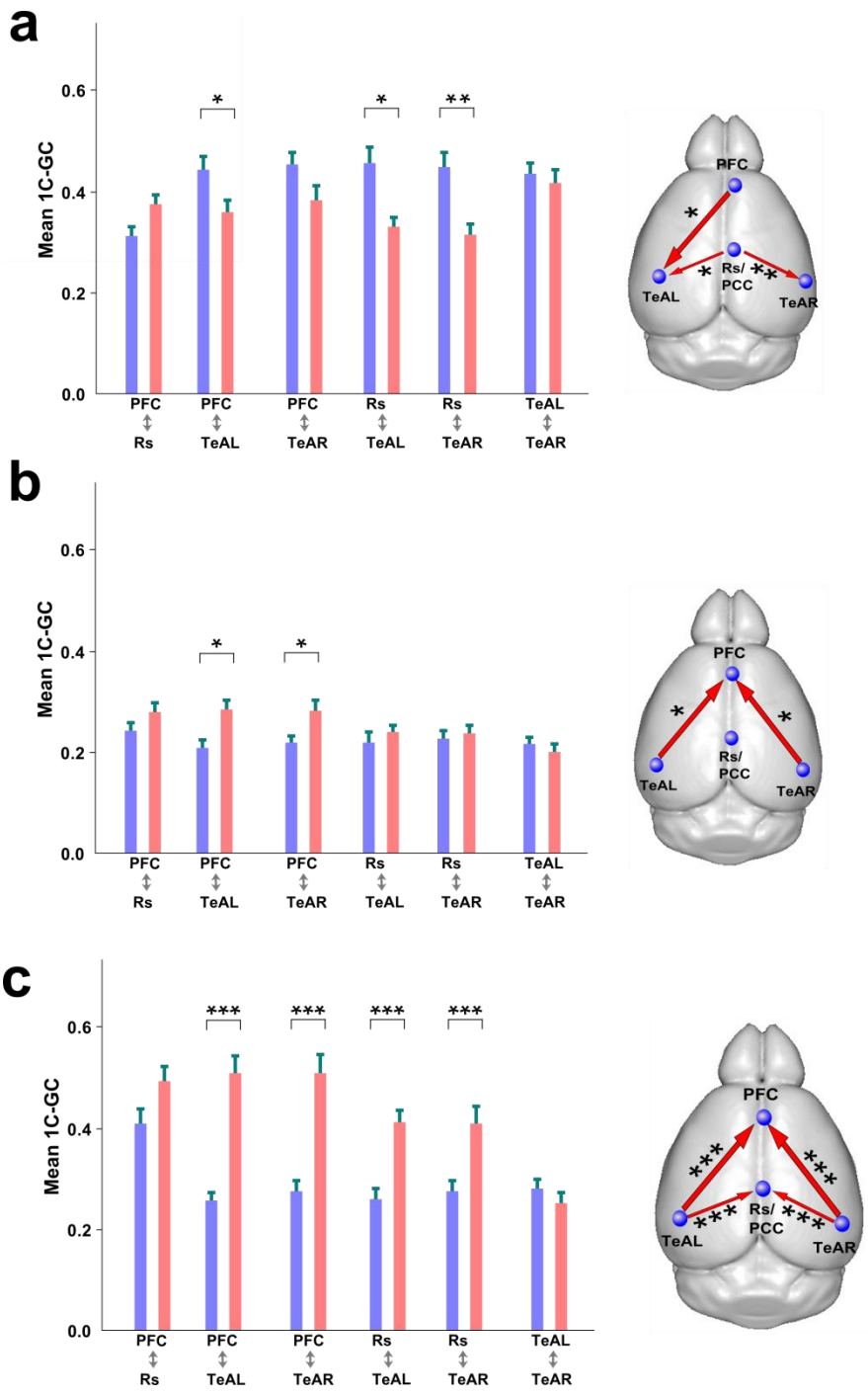

Figure A.1

Figure A.1: Effect of using different kinds of deconvolution on default mode network for 41 mice BOLD data; (a) No deconvolution; (b) with only canonical deconvolution; (c) with canonical deconvolution & time derivative; Each left panel reports the results of 1C-GC (*p<0.05, **p<0.001, *** p<0.0001, asymmetry in GC, paired t-test) and each right panel

represents the corresponding graphical illustration of the dominant directional functional connectivity inferred from GC analysis.

Effect of Global signal regression

A number of previous studies have applied global signal regression to investigate directional connectivity patterns in resting state networks (Wu et al. 2013b, 2013d). However, several other studies did not remove the global signal (Di and Biswal 2014; Razi et al. 2014; Crone et al. 2015). To investigate the effect of Global signal in measuring directional connectivity patterns for resting state networks in mice, we applied one-node conditional Granger causality(1C-GC) over a same set of data collected from 41 subjects with and without global signal regression over the same set of seeds of DMN regions using same deconvolution approach.

Results of this control analysis are reported in Figure A.2 for the 4-node Default mode network (DMN). Although, the overall one-conditional Granger causality (1C-GC) values varied between these two sets of the same data, we found exactly the same pattern of direction connections with and without regressing out the global signal. This suggests that the regression of the global signal is not crucial for the mapping of directional networks with our casualty measures. The reason of this robustness is in our view because the global signal is partly already regressed out in the conditioning over one network node in the 1C-GC calculation, because the global signal correlates with the node we condition upon.

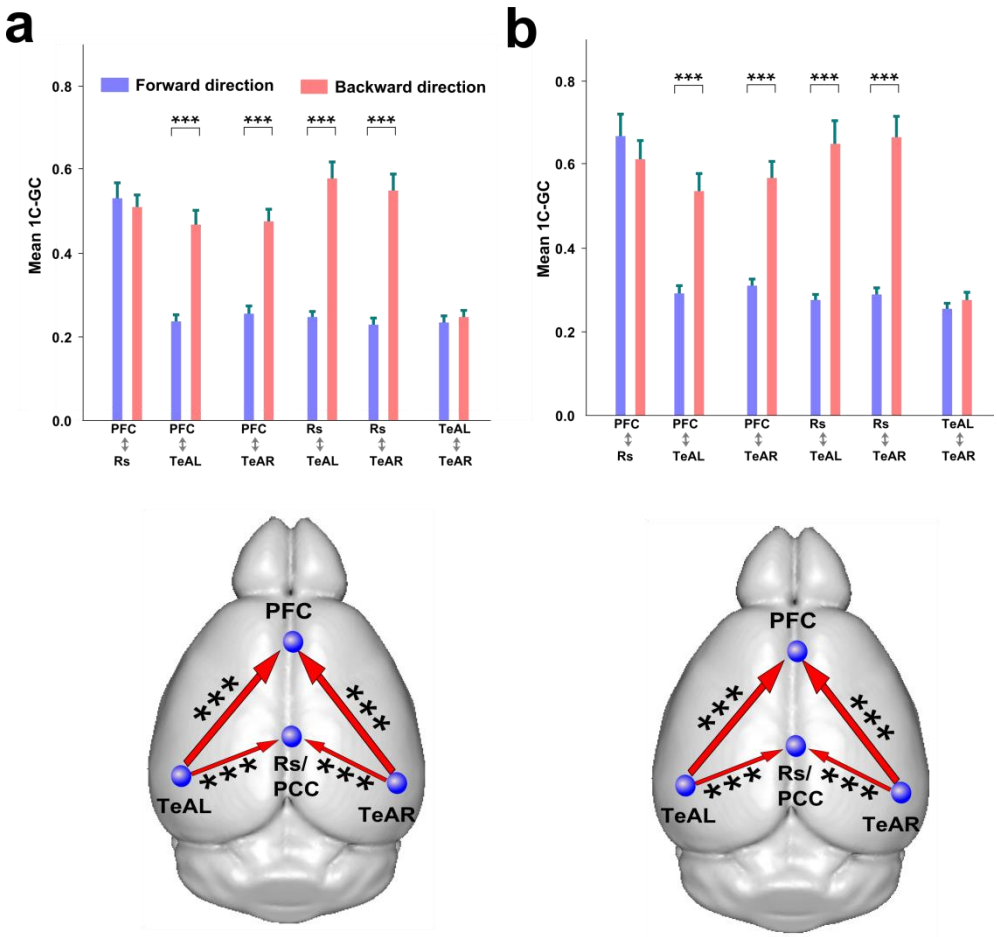

Figure A.2

Figure A.2: Conditional GC without(left panel) and with(right panel) global signal regression of default mode network with 41 mice BOLD data (a) with global signal regression (b) without global signal regression. (DMN 2nd set of ROIs presented in chapter 2). Each top panel reports the results of 1C-GC (*** $p<0.0001$, asymmetry in GC, paired t-test) and each bottom panel represents the corresponding graphical illustration of the dominant directional functional connectivity inferred from GC analysis.

Effect of removing first few data points

Many studies remove the first few slices of functional data to get equilibrium magnetisation of the scanner (Wu et al. 2013c; Di and Biswal 2014; Saleh 2014b; Sforazzini et al. 2014b). The number of slices removed varies from study to study, however removing two to five slices is a common procedure. To check if removing some data points affects our

results, we repeated the 1C-GC calculation in the Default Mode Network (DMN) after removing the first 10, 50 and 100 data points to check the variability of directionality. Interestingly, we did not find any evidence of changing significant dominant directionality (Fig. A.3). Thus our results seem to be robust to the inclusion or exclusion of the slices that may contain non-equilibrium magnetization effects, and see also robust to the number of data points used in the analysis. This latter finding is consistent with the computer simulations of Chapter 2.

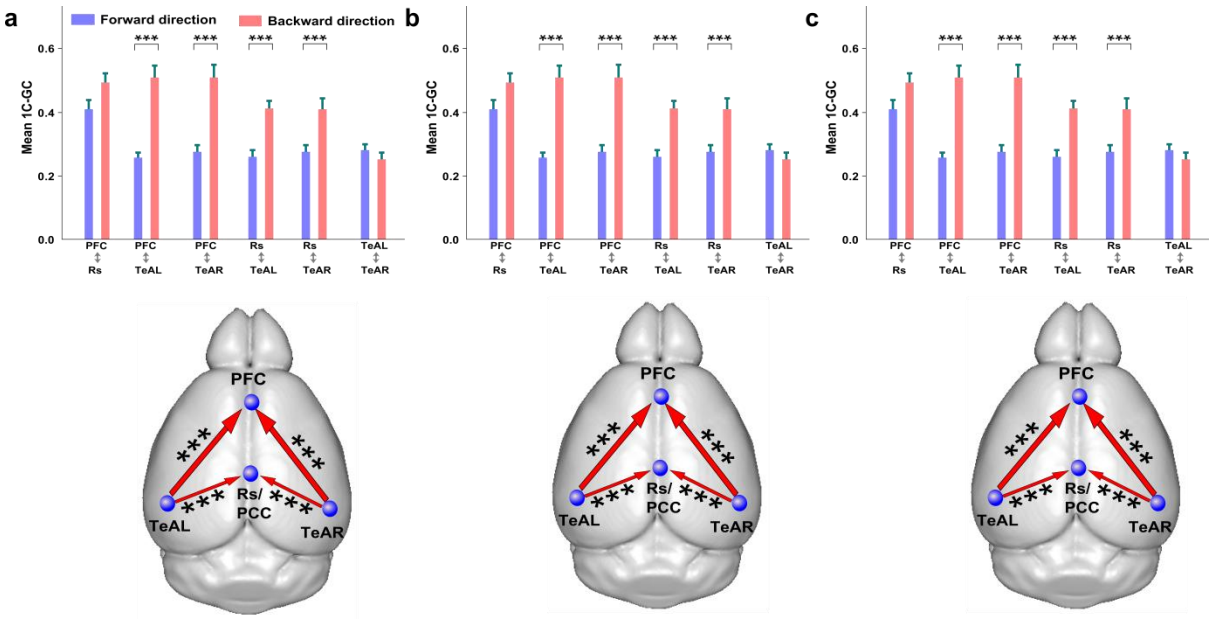

Figure A.3

Figure A.3: Default mode network over 41 BOLD data with one node conditional GC(First set of DMN in chapter 2); after removing first (a) 10 data points, (b) 50 data points and (c) 100 data points. Each top panel reports the results of 1C-GC (*** $p<0.0001$, asymmetry in GC, paired t-test) and each bottom panel represents the corresponding graphical illustration of the dominant directional functional connectivity inferred from GC analysis.

Effect of spatial upsampling of the anatomical templates

In all the cases of our data analysis (chapter 2), we used high spatial resolution anatomical template (198*198*24) to register the data in the preprocessing pipeline. To

understand whether this affects our measure of directional connectivity, we registered our 41 subject BOLD fMRI mice data with a low-resolution template (99*99*24). Then we generated seeds of the 4-node Default Mode Network (DMN) (see Fig. A.4a) and run the Granger Causality analysis as above (Fig. A.4).We found evidence that the proposed dominant directionality patterns were still observed (Fig. A.4b).

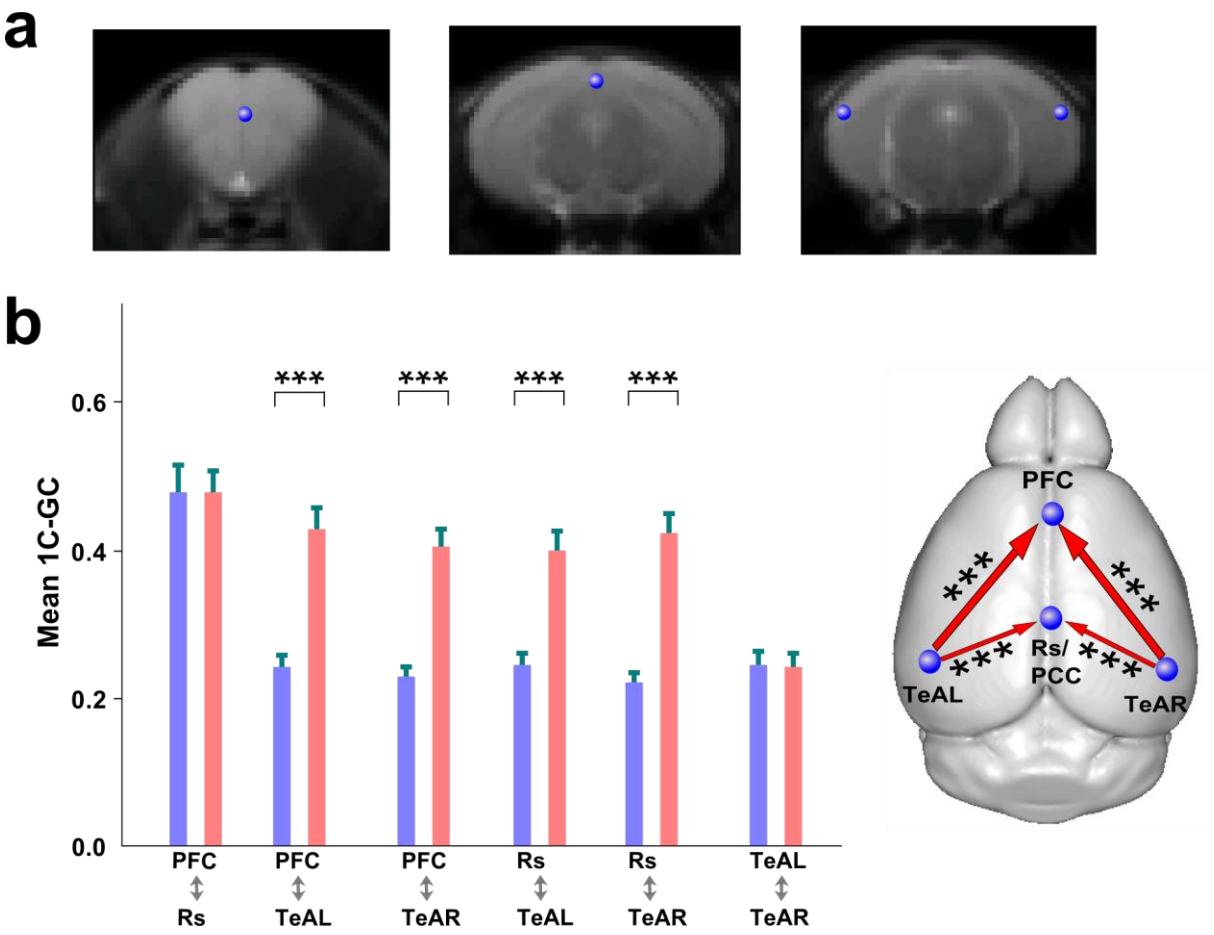

Figure A.4

Figure A.4: DMN with data registered with low resolution template; (a) seed location over anatomical template; (b) left panel represents mean ± SEM of 1C-GC(*** $p<0.0001$, asymmetry in GC, paired t- test) and right panel represents the corresponding graphical illustration of dominant directionality inferred from GC analysis.

Effect of fMRI session length and number of subjects

In Chapter 2, we examined the Granger causality measures obtained from a sample of 41 subjects whose fMRI signals were recorded for 6 minutes. To evaluate whether there could be artefacts in the estimation of GC due to the length of recorded time, we computed 1C-GC again on a separate and smaller number of 14 subjects recorded for a longer time (10 minutes). We found (Fig. A.5 & A.6) that the same structured of directed connections was found with the new datasets with a longer recording time, again stressing the robustness of our results to variations in the experimental conditions.

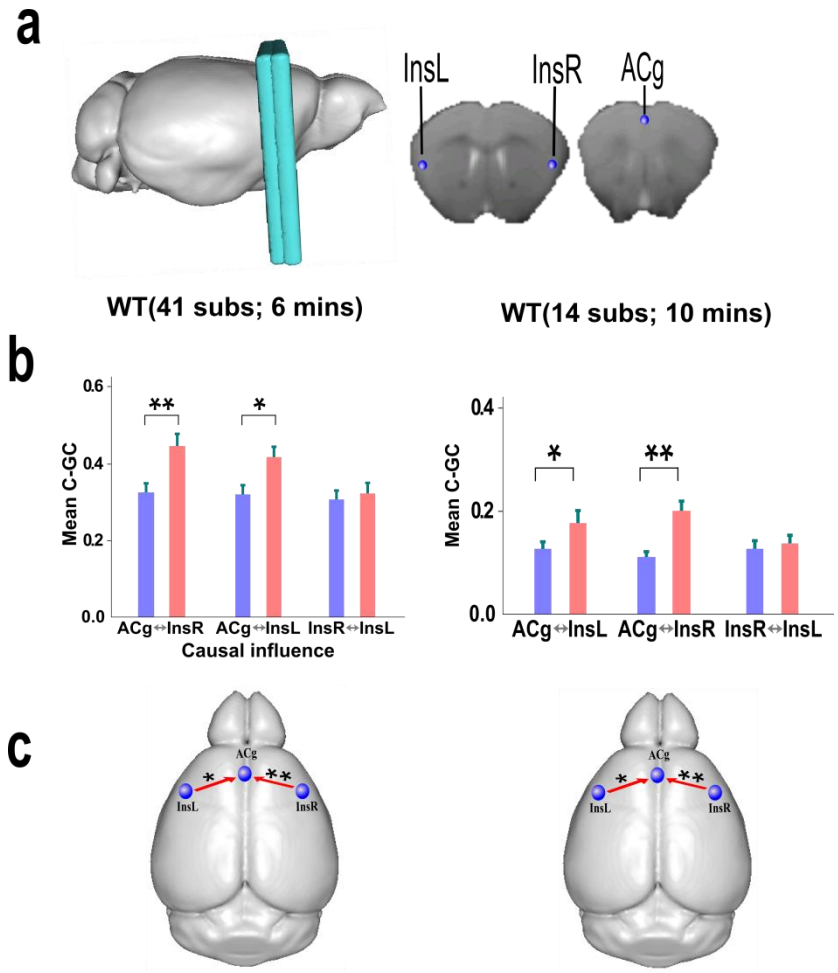

Figure A.5

Figure A.5: Comparison of C-GC results in the salience network obtained with either a sample of 41 subjects whose BOLD signal was recorded for 6 minutes (left panels b& c) or a sample of 14 subjects whose BOLD signal was recorded for 10 minutes (right panels b & c).

The same set of ROIs was used in both conditions; (a), location of salience network ROIs used for GC in original image space and corresponding slices; (b), mean ± SEM of C-GC for all ROI pairs reveal significant directional effects (*p<0.05 & **p<0.001 asymmetry in GC, paired t-test). (c), graphical illustration of the dominant directional functional connectivity inferred from GC analysis.

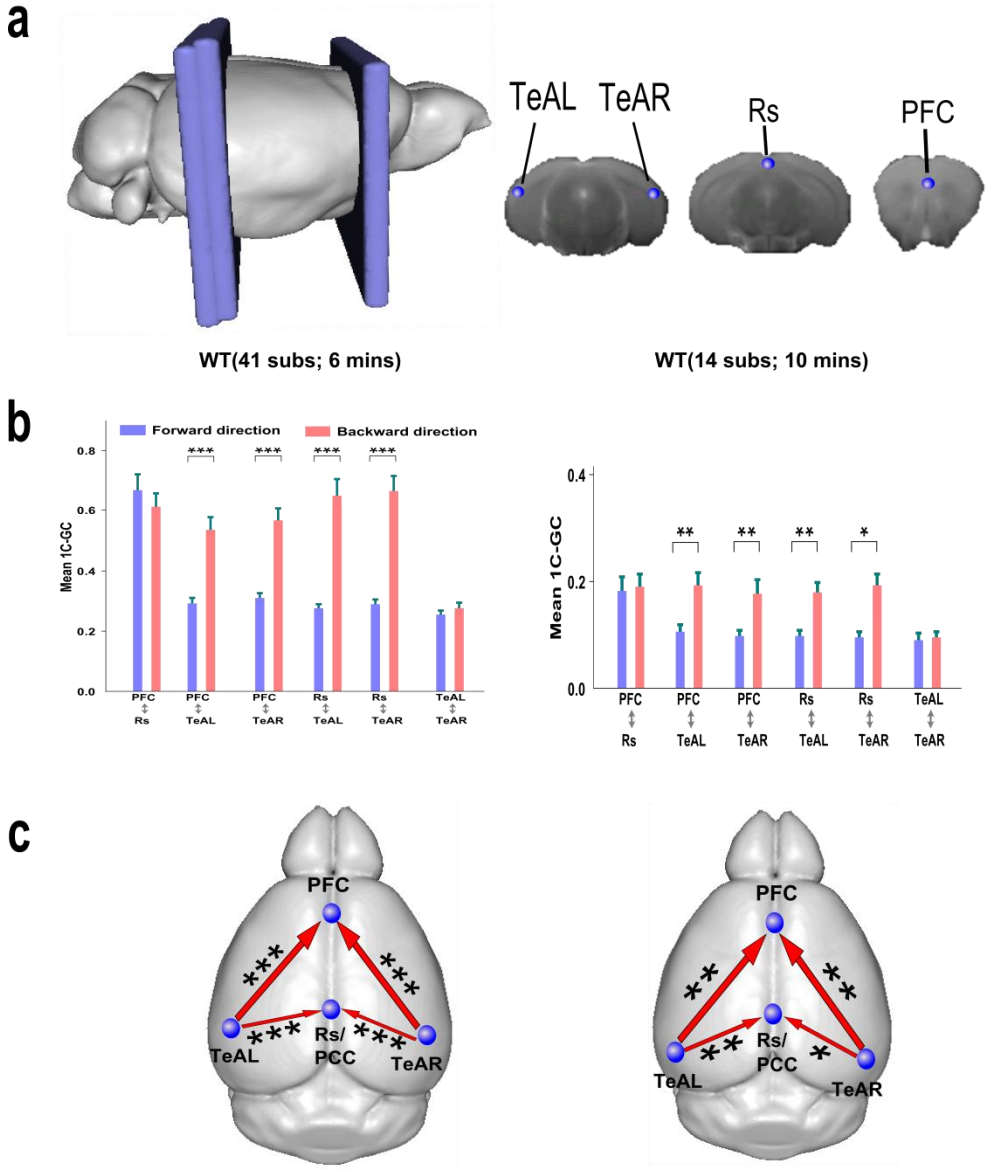

Figure A.6

Figure A.6: Comparison of 1C-GC results in the DMN obtained with either a sample of 41 subjects whose BOLD signal was recorded for 6 minutes (left panels) or a sample of 14 subjects whose BOLD signal was recorded for 10 minutes (right panels). The same set of

ROIs was used in both conditions. (a), location of default mode network ROIs used for GC in original image space and corresponding slices; (b), mean ± SEM of 1C-GC for all ROI pairs reveal significant directional effects (*$p<0.05$ & **$p<0.001$ asymmetry in GC, paired t-test). (c), graphical illustration of the dominant directional functional connectivity inferred from GC analysis.

In summary, session length and number of subjects for fMRI data analysis are important issues especially for directed functional connectivity analysis such as GC. Advanced developments of GC illustrate a way to overcome this limitation(Wen et al. 2013).

Bibliography

Adhikari A, Topiwala MA, Gordon JA. Synchronized activity between the ventral hippocampus and the medial prefrontal cortex during anxiety. Neuron [Internet]. Elsevier; 2010 Jan 28 [cited 2015 Jun 22];65(2):257–69. Available from: http://www.cell.com/article/S0896627309009799/fulltext

Amblard P-O, Michel O. The Relation between Granger Causality and Directed Information Theory: A Review. Entropy [Internet]. 2012 Dec 28 [cited 2014 Sep 5];15(1):113–43. Available from: http://www.mdpi.com/1099-4300/15/1/113/

Anagnostou E, Taylor MJ. Review of neuroimaging in autism spectrum disorders: what have we learned and where we go from here. Mol Autism [Internet]. 2011 Jan [cited 2015 Jul 18];2(1):4. Available from: http://www.pubmedcentral.nih.gov/articlerender.fcgi?artid=3102613&tool=pmcentrez&rendertype=abstract

Ancona N, Marinazzo D, Stramaglia S. Radial basis function approach to nonlinear Granger causality of time series. Phys Rev E [Internet]. 2004 Nov [cited 2014 Aug 8];70(5):056221. Available from: http://link.aps.org/doi/10.1103/PhysRevE.70.056221

Ashrafulla S, Haldar JP, Joshi AA, Leahy RM. Canonical Granger causality between regions of interest. Neuroimage [Internet]. 2013 Dec [cited 2014 Aug 22];83:189–99. Available from: http://www.pubmedcentral.nih.gov/articlerender.fcgi?artid=4026328&tool=pmcentrez&rendertype=abstract

Badre D. Cognitive control, hierarchy, and the rostro-caudal organization of the frontal lobes. Trends Cogn Sci [Internet]. 2008 May [cited 2014 Nov 27];12(5):193–200. Available from: http://www.ncbi.nlm.nih.gov/pubmed/18403252

Barnett L, Seth AK. Behaviour of Granger causality under filtering: theoretical invariance and practical application. J Neurosci Methods [Internet]. 2011 Oct 15 [cited 2014 Sep 6];201(2):404–19. Available from: http://www.ncbi.nlm.nih.gov/pubmed/21864571

Barnett L, Seth AK. The MVGC multivariate Granger causality toolbox: a new approach to Granger-causal inference. J Neurosci Methods [Internet]. Elsevier B.V.; 2014 Feb 15 [cited 2014 Jul 15];223:50–68. Available from: http://www.ncbi.nlm.nih.gov/pubmed/24200508

Beckmann CF, DeLuca M, Devlin JT, Smith SM. Investigations into resting-state connectivity using independent component analysis. Philos Trans R Soc Lond B Biol Sci [Internet]. 2005 May 29 [cited 2014 Jul 10];360(1457):1001–13. Available from: http://rstb.royalsocietypublishing.org/content/360/1457/1001.short

Bifone A, Gozzi A. Functional and pharmacological MRI in understanding brain function at a systems level. Curr Top Behav Neurosci [Internet]. 2011 Jan [cited 2014 Sep 6];7:323–57. Available from: http://www.ncbi.nlm.nih.gov/pubmed/21225416

Biswal B, Yetkin FZ, Haughton VM, Hyde JS. Functional Connectivity in the Motor Cortex of Resting.

(9):537–41.

Bitan T, Lifshitz A, Breznitz Z, Booth JR. Bidirectional connectivity between hemispheres occurs at multiple levels in language processing but depends on sex. J Neurosci [Internet]. 2010 Sep 1 [cited 2014 Sep 6];30(35):11576–85. Available from: http://www.jneurosci.org/content/30/35/11576.short

Bogue M. Mouse Phenome Project: understanding human biology through mouse genetics and genomics. J Appl Physiol [Internet]. 2003 Oct 1 [cited 2014 Sep 6];95(4):1335–7. Available from: http://jap.physiology.org/content/95/4/1335

Bressler SL, Seth AK. Wiener-Granger causality: a well established methodology. Neuroimage [Internet]. Elsevier Inc.; 2011 Sep 15 [cited 2014 Jul 10];58(2):323–9. Available from: http://www.ncbi.nlm.nih.gov/pubmed/20202481

Brockmann MD, Pöschel B, Cichon N, Hanganu-Opatz IL. Coupled oscillations mediate directed interactions between prefrontal cortex and hippocampus of the neonatal rat. Neuron [Internet]. 2011 Jul 28 [cited 2015 Mar 24];71(2):332–47. Available from: http://www.sciencedirect.com/science/article/pii/S0896627311004983

Chen T, Michels L, Supekar K, Kochalka J, Ryali S, Menon V. Role of the anterior insular cortex in integrative causal signaling during multisensory auditory-visual attention. Eur J Neurosci [Internet]. 2015 Jan [cited 2015 Aug 8];41(September 2014):264–74. Available from: http://www.ncbi.nlm.nih.gov/pubmed/25352218

Chicharro D, Panzeri S. Algorithms of causal inference for the analysis of effective connectivity among brain regions. Front Neuroinform [Internet]. Frontiers; 2014 Jan 2 [cited 2015 Oct 29];8:64. Available from: http://journal.frontiersin.org/article/10.3389/fninf.2014.00064/abstract

Clemm von Hohenberg C, Wigand MC, Kubicki M, Leicht G, Giegling I, Karch S, et al. CNTNAP2 polymorphisms and structural brain connectivity: a diffusion-tensor imaging study. J Psychiatr Res [Internet]. 2013 Oct [cited 2015 Oct 29];47(10):1349–56. Available from: http://www.pubmedcentral.nih.gov/articlerender.fcgi?artid=3780783&tool=pmcentrez&rendertype=abstract

Cordes D, Haughton VM, Arfanakis K, Wendt GJ, Turski P a, Moritz CH, et al. Mapping functionally related regions of brain with functional connectivity MR imaging. AJNR Am J Neuroradiol [Internet]. 2000 Oct;21(9):1636–44. Available from: http://www.ncbi.nlm.nih.gov/pubmed/11039342

Crone JS, Schurz M, Höller Y, Bergmann J, Monti M, Schmid E, et al. Impaired consciousness is linked to changes in effective connectivity of the posterior cingulate cortex within the default mode network. Neuroimage [Internet]. 2015 Jan 22 [cited 2015 Jan 30]; Available from: http://www.sciencedirect.com/science/article/pii/S1053811915000531

David O. fMRI connectivity, meaning and empiricism Comments on: Roebroeck et al. The identification of interacting networks in the brain using fMRI: model selection, causality and deconvolution. Neuroimage [Internet]. Elsevier Inc.; 2011 Sep 15 [cited 2014 Sep 5];58(2):306–

9; author reply 310–1. Available from: http://www.ncbi.nlm.nih.gov/pubmed/19892020

Deshpande G, Hu X. Investigating effective brain connectivity from fMRI data: past findings and current issues with reference to Granger causality analysis. Brain Connect [Internet]. 2012 Jan [cited 2014 Aug 9];2(5):235–45. Available from: http://www.pubmedcentral.nih.gov/articlerender.fcgi?artid=3621319&tool=pmcentrez&rendertype=abstract

Deshpande G, Santhanam P, Hu X. Instantaneous and causal connectivity in resting state brain networks derived from functional MRI data. Neuroimage [Internet]. Elsevier Inc.; 2011 Jan 15 [cited 2014 Sep 5];54(2):1043–52. Available from: http://www.sciencedirect.com/science/article/pii/S105381191001205X

Deshpande G, Sathian K, Hu X. Effect of hemodynamic variability on Granger causality analysis of fMRI. Neuroimage [Internet]. 2010 Sep [cited 2014 Sep 6];52(3):884–96. Available from: http://www.sciencedirect.com/science/article/pii/S1053811909012464

Detto M, Molini A, Katul G, Stoy P, Palmroth S, Baldocchi D. Causality and persistence in ecological systems: a nonparametric spectral granger causality approach. Am Nat [Internet]. 2012 Apr [cited 2014 Aug 8];179(4):524–35. Available from: http://www.ncbi.nlm.nih.gov/pubmed/22437181

Di X, Biswal BB. Identifying the default mode network structure using dynamic causal modeling on resting-state functional magnetic resonance imaging. Neuroimage [Internet]. Elsevier B.V.; 2014 Feb 1 [cited 2014 Jul 26];86:53–9. Available from: http://www.ncbi.nlm.nih.gov/pubmed/23927904

Ding M, Chen Y, Bressler SL. Granger Causality: Basic Theory and Application to Neuroscience. 2006 Aug 23 [cited 2014 Aug 17];(February). Available from: http://arxiv.org/abs/q-bio/0608035

Ferrari L, Turrini G, Crestan V, Bertani S, Cristofori P, Bifone A, et al. A robust experimental protocol for pharmacological fMRI in rats and mice. J Neurosci Methods [Internet]. 2012 Feb 15 [cited 2014 Sep 6];204(1):9–18. Available from: http://www.ncbi.nlm.nih.gov/pubmed/22068031

Fox MD, Snyder AZ, Vincent JL, Corbetta M, Van Essen DC, Raichle ME. The human brain is intrinsically organized into dynamic, anticorrelated functional networks. Proc Natl Acad Sci U S A [Internet]. 2005 Jul 5 [cited 2014 Jul 10];102(27):9673–8. Available from: http://www.pnas.org/content/102/27/9673.full

Friston K, Moran R, Seth AK. Analysing connectivity with Granger causality and dynamic causal modelling. Curr Opin Neurobiol [Internet]. Elsevier Ltd; 2013 Apr [cited 2014 Jul 10];23(2):172–8. Available from: http://www.pubmedcentral.nih.gov/articlerender.fcgi?artid=3925802&tool=pmcentrez&rendertype=abstract

Friston KJ. Functional and effective connectivity: a review. Brain Connect [Internet]. 2011 Jan [cited 2014 Jul 9];1(1):13–36. Available from: http://www.ncbi.nlm.nih.gov/pubmed/22432952

Friston KJ, Bastos AM, Oswal A, van Wijk B, Richter C, Litvak V. Granger causality revisited.

Neuroimage [Internet]. The Authors; 2014a Jul 5 [cited 2014 Jul 10];101:796–808. Available from: http://www.pubmedcentral.nih.gov/articlerender.fcgi?artid=4176655&tool=pmcentrez&rendertype=abstract

Friston KJ, Harrison L, Penny W. Dynamic causal modelling. Neuroimage [Internet]. 2003 Aug [cited 2014 Jul 10];19(4):1273–302. Available from: http://linkinghub.elsevier.com/retrieve/pii/S1053811903002027

Friston KJ, Kahan J, Biswal B, Razi A. A DCM for resting state fMRI. Neuroimage [Internet]. The Authors; 2014b Jul 1 [cited 2014 Aug 25];94:396–407. Available from: http://www.pubmedcentral.nih.gov/articlerender.fcgi?artid=4073651&tool=pmcentrez&rendertype=abstract

Friston KJ, Kahan J, Razi A, Stephan KE, Sporns O. On nodes and modes in resting state fMRI. Neuroimage [Internet]. 2014c May 24 [cited 2014 Jul 21];99:533–47. Available from: http://www.sciencedirect.com/science/article/pii/S1053811914004212

Gautama T, Hulle V, Gasthuisberg C, Van Hulle MM. Surrogate-based test for Granger causality. 2003 IEEE XIII Work Neural Networks Signal Process (IEEE Cat No03TH8718) [Internet]. IEEE; 2003 [cited 2014 Oct 13]. p. 799–808. Available from: http://ieeexplore.ieee.org/lpdocs/epic03/wrapper.htm?arnumber=1318079

Goebel R, Roebroeck A, Kim D-S, Formisano E. Investigating directed cortical interactions in time-resolved fMRI data using vector autoregressive modeling and Granger causality mapping. Magn Reson Imaging [Internet]. 2003 Dec [cited 2014 Sep 6];21(10):1251–61. Available from: http://linkinghub.elsevier.com/retrieve/pii/S0730725X03003370

Göttlich M, Münte TF, Heldmann M, Kasten M, Hagenah J, Krämer UM. Altered resting state brain networks in Parkinson's disease. PLoS One [Internet]. 2013 Jan [cited 2014 Aug 6];8(10):e77336. Available from: http://www.pubmedcentral.nih.gov/articlerender.fcgi?artid=3810472&tool=pmcentrez&rendertype=abstract

Gozzi A, Ceolin L, Schwarz A, Reese T, Bertani S, Crestan V, et al. A multimodality investigation of cerebral hemodynamics and autoregulation in pharmacological MRI. Magn Reson Imaging [Internet]. 2007 Jul [cited 2015 Jun 10];25(6):826–33. Available from: http://www.sciencedirect.com/science/article/pii/S0730725X07002147

Gozzi A, Jain A, Giovannelli A, Giovanelli A, Bertollini C, Crestan V, et al. A neural switch for active and passive fear. Neuron [Internet]. 2010 Aug 26 [cited 2014 Aug 23];67(4):656–66. Available from: http://www.sciencedirect.com/science/article/pii/S0896627310005465

De Groof G, Jonckers E, Güntürkün O, Denolf P, Van Auderkerke J, Van der Linden A. Functional MRI and functional connectivity of the visual system of awake pigeons. Behav Brain Res [Internet]. 2013 Feb 15 [cited 2014 Sep 6];239:43–50. Available from: http://www.sciencedirect.com/science/article/pii/S0166432812006948

Hacker CD, Laumann TO, Szrama NP, Baldassarre A, Snyder AZ, Leuthardt EC, et al. Resting state

network estimation in individual subjects. Neuroimage [Internet]. Elsevier Inc.; 2013 Nov 15 [cited 2014 Aug 24];82:616–33. Available from: http://www.ncbi.nlm.nih.gov/pubmed/23735260

Holroyd CB, McClure SM. Hierarchical control over effortful behavior by rodent medial frontal cortex: A computational model. 2014;

Honey CJ, Kötter R, Breakspear M, Sporns O. Network structure of cerebral cortex shapes functional connectivity on multiple time scales. Proc Natl Acad Sci U S A [Internet]. 2007 Jun 12;104(24):10240–5. Available from: http://www.pubmedcentral.nih.gov/articlerender.fcgi?artid=1891224&tool=pmcentrez&rendertype=abstract

Hoover WB, Vertes RP. Anatomical analysis of afferent projections to the medial prefrontal cortex in the rat. Brain Struct Funct [Internet]. 2007 Sep [cited 2014 Dec 2];212(2):149–79. Available from: http://www.ncbi.nlm.nih.gov/pubmed/17717690

Hu M, Liang H. A copula approach to assessing Granger causality. Neuroimage [Internet]. Elsevier B.V.; 2014 Oct 15 [cited 2014 Sep 5];100:125–34. Available from: http://www.ncbi.nlm.nih.gov/pubmed/24945669

Hurley KM, Herbert H, Moga MM, Saper CB. Efferent projections of the infralimbic cortex of the rat. J Comp Neurol [Internet]. 1991 Jun 8 [cited 2015 Aug 8];308(2):249–76. Available from: http://www.ncbi.nlm.nih.gov/pubmed/1716270

Hutchison RM, Mirsattari SM, Jones CK, Gati JS, Leung LS. Functional networks in the anesthetized rat brain revealed by independent component analysis of resting-state FMRI. J Neurophysiol [Internet]. 2010 Jun [cited 2014 Sep 5];103(6):3398–406. Available from: http://www.ncbi.nlm.nih.gov/pubmed/20410359

Jiao Q, Lu G, Zhang Z, Zhong Y, Wang Z, Guo Y, et al. Granger causal influence predicts BOLD activity levels in the default mode network. Hum Brain Mapp [Internet]. 2011 Jan [cited 2014 Sep 10];32(1):154–61. Available from: http://www.ncbi.nlm.nih.gov/pubmed/21157880

Joel SE, Caffo BS, van Zijl PCM, Pekar JJ. On the relationship between seed-based and ICA-based measures of functional connectivity. Magn Reson Med [Internet]. 2011 Sep [cited 2014 Aug 29];66(3):644–57. Available from: http://www.pubmedcentral.nih.gov/articlerender.fcgi?artid=3130118&tool=pmcentrez&rendertype=abstract

Jolliffe I. Principal Component Analysis [Internet]. John Wiley & Sons, Ltd; 2005. Available from: http://dx.doi.org/10.1002/0470013192.bsa501

Kamiński M, Ding M, Truccolo WA, Bressler SL. Evaluating causal relations in neural systems: granger causality, directed transfer function and statistical assessment of significance. Biol Cybern [Internet]. 2001 Aug [cited 2015 Apr 23];85(2):145–57. Available from: http://www.ncbi.nlm.nih.gov/pubmed/11508777

Lang EW, Tomé a M, Keck IR, Górriz-Sáez JM, Puntonet CG. Brain connectivity analysis: a short

survey. Comput Intell Neurosci [Internet]. 2012 Jan [cited 2014 Aug 18];2012(iii):412512. Available from: http://www.pubmedcentral.nih.gov/articlerender.fcgi?artid=3477528&tool=pmcentrez&rendertype=abstract

Lee MH, Smyser CD, Shimony JS. Resting-state fMRI: a review of methods and clinical applications. AJNR Am J Neuroradiol [Internet]. 2013 Oct;34(10):1866–72. Available from: http://www.ncbi.nlm.nih.gov/pubmed/22936095

Li B, Wang X, Yao S, Hu D, Friston K. Task-Dependent Modulation of Effective Connectivity within the Default Mode Network. Front Psychol [Internet]. 2012 Jan [cited 2015 Feb 25];3:206. Available from: http://www.pubmedcentral.nih.gov/articlerender.fcgi?artid=3381220&tool=pmcentrez&rendertype=abstract

Liao W, Marinazzo D, Pan Z, Gong Q, Chen H. Kernel Granger causality mapping effective connectivity on FMRI data. IEEE Trans Med Imaging [Internet]. 2009 Nov;28(11):1825–35. Available from: http://www.ncbi.nlm.nih.gov/pubmed/19709972

Liu Y, Wu X, Zhang J, Guo X, Long Z, Yao L. Altered effective connectivity model in the default mode network between bipolar and unipolar depression based on resting-state fMRI. J Affect Disord [Internet]. 2015 Aug 15 [cited 2015 Jun 16];182:8–17. Available from: http://www.sciencedirect.com/science/article/pii/S0165032715002244

Liu Z, Zhang Y, Bai L, Yan H, Dai R, Zhong C, et al. Investigation of the effective connectivity of resting state networks in Alzheimer's disease: a functional MRI study combining independent components analysis and multivariate Granger causality analysis. NMR Biomed [Internet]. 2012 Dec [cited 2014 Sep 5];25(12):1311–20. Available from: http://www.ncbi.nlm.nih.gov/pubmed/22505275

Logothetis NK. What we can do and what we cannot do with fMRI. Nature [Internet]. Macmillan Publishers Limited. All rights reserved; 2008 Jun 12 [cited 2014 Jul 9];453(7197):869–78. Available from: http://dx.doi.org/10.1038/nature06976

Lu H, Zou Q, Gu H, Raichle ME, Stein E a, Yang Y. Rat brains also have a default mode network. Proc Natl Acad Sci U S A [Internet]. 2012 Mar 6 [cited 2014 Jul 10];109(10):3979–84. Available from: http://www.pubmedcentral.nih.gov/articlerender.fcgi?artid=3309754&tool=pmcentrez&rendertype=abstract

Lütkepohl H. New introduction to multiple time series analysis. Berlin: Springer-Verlag. 2005;

Marinazzo D, Pellicoro M, Stramaglia S. Kernel Method for Nonlinear Granger Causality. Phys Rev Lett [Internet]. 2008 Apr [cited 2014 Sep 6];100(14):144103. Available from: http://link.aps.org/doi/10.1103/PhysRevLett.100.144103

Miao X, Wu X, Li R, Chen K, Yao L. Altered connectivity pattern of hubs in default-mode network with Alzheimer's disease: an Granger causality modeling approach. PLoS One [Internet]. 2011 Jan [cited 2014 Sep 19];6(10):e25546. Available from: http://www.pubmedcentral.nih.gov/articlerender.fcgi?artid=3191142&tool=pmcentrez&rende

rtype=abstract

Mingoia G, Wagner G, Langbein K, Maitra R, Smesny S, Dietzek M, et al. Default mode network activity in schizophrenia studied at resting state using probabilistic ICA. Schizophr Res [Internet]. Elsevier B.V.; 2012 Jul [cited 2014 Aug 28];138(2-3):143–9. Available from: http://www.ncbi.nlm.nih.gov/pubmed/22578721

Nalatore H, Ding M, Rangarajan G. Mitigating the effects of measurement noise on Granger causality. Phys Rev E [Internet]. 2007 Mar [cited 2014 Sep 6];75(3):031123. Available from: http://link.aps.org/doi/10.1103/PhysRevE.75.031123

Ogawa S, Lee TM, Stepnoski R, Chen W, Zhu XH, Ugurbil K. An approach to probe some neural systems interaction by functional MRI at neural time scale down to milliseconds. Proc Natl Acad Sci U S A [Internet]. 2000 Sep 26;97(20):11026–31. Available from: http://www.pubmedcentral.nih.gov/articlerender.fcgi?artid=27142&tool=pmcentrez&rendertype=abstract

Orth M, Bravo E, Barter L, Carstens E, Antognini JF. The differential effects of halothane and isoflurane on electroencephalographic responses to electrical microstimulation of the reticular formation. Anesth Analg [Internet]. 2006 Jun [cited 2015 Aug 8];102(6):1709–14. Available from: http://www.ncbi.nlm.nih.gov/pubmed/16717314

Patel RS, Bowman FD, Rilling JK. A Bayesian approach to determining connectivity of the human brain. Hum Brain Mapp [Internet]. 2006 Mar [cited 2015 Jun 30];27(3):267–76. Available from: http://doi.wiley.com/10.1002/hbm.20182

Peñagarikano O, Abrahams BS, Herman EI, Winden KD, Gdalyahu A, Dong H, et al. Absence of CNTNAP2 leads to epilepsy, neuronal migration abnormalities, and core autism-related deficits. Cell [Internet]. 2011 Sep 30 [cited 2015 Apr 23];147(1):235–46. Available from: http://www.pubmedcentral.nih.gov/articlerender.fcgi?artid=3390029&tool=pmcentrez&rendertype=abstract

Penke L, Deary IJ. Some guidelines for structural equation modelling in cognitive neuroscience: the case of Charlton et al.'s study on white matter integrity and cognitive ageing. Neurobiol Aging [Internet]. 2010 Sep [cited 2014 Sep 6];31(9):1656–60; discussion 1561–6. Available from: http://www.sciencedirect.com/science/article/pii/S0197458009004047

Razi A, Kahan J, Rees G, Friston KJ. Construct validation of a DCM for resting state fMRI. Neuroimage [Internet]. 2014 Nov [cited 2014 Nov 25];106:1–14. Available from: http://www.sciencedirect.com/science/article/pii/S1053811914009446

Rilling JK, Barks SK, Parr L a, Preuss TM, Faber TL, Pagnoni G, et al. A comparison of resting-state brain activity in humans and chimpanzees. Proc Natl Acad Sci U S A [Internet]. 2007 Oct 23;104(43):17146–51. Available from: http://www.pubmedcentral.nih.gov/articlerender.fcgi?artid=2040430&tool=pmcentrez&rendertype=abstract

Roebroeck A, Formisano E, Goebel R. Mapping directed influence over the brain using Granger causality and fMRI. Neuroimage [Internet]. 2005 Mar [cited 2014 Jul 11];25(1):230–42.

Available from: http://www.sciencedirect.com/science/article/pii/S1053811904006688

Roebroeck A, Formisano E, Goebel R. Reply to Friston and David. Neuroimage [Internet]. 2011a Sep [cited 2015 Feb 2];58(2):310–1. Available from: http://www.sciencedirect.com/science/article/pii/S1053811909011483

Roebroeck A, Formisano E, Goebel R. The identification of interacting networks in the brain using fMRI: Model selection, causality and deconvolution. Neuroimage [Internet]. 2011b Sep 15 [cited 2015 Jan 1];58(2):296–302. Available from: http://www.sciencedirect.com/science/article/pii/S1053811909010155

Roebroeck A, Formisano E, Goebel R, David O, Friston K, Roebroeck A, et al. The identification of interacting networks in the brain using fMRI: Model selection, causality and deconvolution. Neuroimage [Internet]. Elsevier Inc.; 2011c Sep 15 [cited 2014 Aug 29];58(2):296–302. Available from: http://www.ncbi.nlm.nih.gov/pubmed/19786106

Saleh I. fMRI resting state time series causality: comparison of Granger causality and phase slope index. Int J Res Med Sci [Internet]. 2014a [cited 2014 Sep 5];2(1):47. Available from: http://www.scopemed.org/?mno=47473

Saleh IEH. fMRI resting state time series causality: comparison of Granger causality and phase slope index. Int J Res Med Sci [Internet]. 2014b Jan 1 [cited 2014 Sep 5];2(1):47. Available from: http://www.scopemed.org/?mno=47473

Schreiber T, Schmitz A. Surrogate time series. Phys D Nonlinear Phenom [Internet]. 2000 Aug [cited 2014 Oct 13];142(3-4):346–82. Available from: http://www.sciencedirect.com/science/article/pii/S0167278900000439

Schwarz AJ, Gass N, Sartorius A, Zheng L, Spedding M, Schenker E, et al. The low-frequency blood oxygenation level-dependent functional connectivity signature of the hippocampal-prefrontal network in the rat brain. Neuroscience [Internet]. 2013 Jan 3 [cited 2015 Jun 10];228:243–58. Available from: http://www.sciencedirect.com/science/article/pii/S0306452212010470

Schwarz AJ, Gozzi A, Bifone A. Community structure and modularity in networks of correlated brain activity. Magn Reson Imaging [Internet]. 2008 Sep [cited 2014 Sep 6];26(7):914–20. Available from: http://www.sciencedirect.com/science/article/pii/S0730725X08000829

Scott-Van Zeeland AA, Abrahams BS, Alvarez-Retuerto AI, Sonnenblick LI, Rudie JD, Ghahremani D, et al. Altered Functional Connectivity in Frontal Lobe Circuits Is Associated with Variation in the Autism Risk Gene CNTNAP2. Sci Transl Med [Internet]. 2010 Nov 3 [cited 2015 Oct 15];2(56):56ra80–56ra80. Available from: http://www.pubmedcentral.nih.gov/articlerender.fcgi?artid=3065863&tool=pmcentrez&rendertype=abstract

Seeley WW, Menon V, Schatzberg AF, Keller J, Glover GH, Kenna H, et al. Dissociable intrinsic connectivity networks for salience processing and executive control. J Neurosci [Internet]. 2007 Feb 28 [cited 2014 Jul 9];27(9):2349–56. Available from: http://www.pubmedcentral.nih.gov/articlerender.fcgi?artid=2680293&tool=pmcentrez&rendertype=abstract

Seth AK. A MATLAB toolbox for Granger causal connectivity analysis. J Neurosci Methods [Internet]. 2010 Feb 15 [cited 2014 Jul 15];186(2):262–73. Available from: http://www.ncbi.nlm.nih.gov/pubmed/19961876

Seth AK, Barrett AB, Barnett L. Granger Causality Analysis in Neuroscience and Neuroimaging. J Neurosci [Internet]. 2015 Feb 25 [cited 2015 Feb 26];35(8):3293–7. Available from: http://www.jneurosci.org/content/35/8/3293.full

Seth AK, Chorley P, Barnett LC. Granger causality analysis of fMRI BOLD signals is invariant to hemodynamic convolution but not downsampling. Neuroimage [Internet]. Elsevier Inc.; 2013 Jan 15 [cited 2014 Aug 28];65:540–55. Available from: http://www.ncbi.nlm.nih.gov/pubmed/23036449

Sforazzini F, Bertero A, Dodero L, David G, Galbusera A, Scattoni ML, et al. Altered functional connectivity networks in acallosal and socially impaired BTBR mice. Brain Struct Funct [Internet]. 2014a;(Shevell 2002). Available from: http://link.springer.com/10.1007/s00429-014-0948-9

Sforazzini F, Schwarz AJ, Galbusera A, Bifone A, Gozzi A. Distributed BOLD and CBV-weighted resting-state networks in the mouse brain. Neuroimage [Internet]. Elsevier Inc.; 2014b Feb 15 [cited 2014 Sep 5];87:403–15. Available from: http://www.ncbi.nlm.nih.gov/pubmed/24080504

Shah D, Blockx I, Keliris GA, Kara F, Jonckers E, Verhoye M, et al. Cholinergic and serotonergic modulations differentially affect large-scale functional networks in the mouse brain. Brain Struct Funct [Internet]. 2015 Jul 21 [cited 2015 Jul 23]; Available from: http://www.ncbi.nlm.nih.gov/pubmed/26195064

Shim WH, Baek K, Kim JK, Chae Y, Suh J-Y, Rosen BR, et al. Frequency distribution of causal connectivity in rat sensorimotor network: resting-state fMRI analyses. J Neurophysiol [Internet]. 2013 Jan [cited 2014 Sep 5];109(1):238–48. Available from: http://www.ncbi.nlm.nih.gov/pubmed/23019001

Silfverhuth MJ, Remes J, Starck T, Nikkinen J, Veijola J, Tervonen O, et al. Directional connectivity of resting state human fMRI data using cascaded ICA-PDC analysis. Acta Radiol [Internet]. 2011 Nov 1 [cited 2015 Jun 5];52(9):1037–42. Available from: http://www.ncbi.nlm.nih.gov/pubmed/22045722

Sims CA. Money, Income, and Causality. Am Econ Rev. 1972;62(4):540–52.

Smith SM. The future of FMRI connectivity. Neuroimage [Internet]. Elsevier Inc.; 2012 Aug 15 [cited 2014 Jul 15];62(2):1257–66. Available from: http://www.ncbi.nlm.nih.gov/pubmed/22248579

Smith SM, Miller KL, Salimi-Khorshidi G, Webster M, Beckmann CF, Nichols TE, et al. Network modelling methods for FMRI. Neuroimage [Internet]. Elsevier Inc.; 2011 Jan 15 [cited 2014 Jul 10];54(2):875–91. Available from: http://www.sciencedirect.com/science/article/pii/S1053811910011602

Sridharan D, Levitin DJ, Menon V. A critical role for the right fronto-insular cortex in switching between central-executive and default-mode networks. Proc Natl Acad Sci U S A [Internet].

2008 Aug 26 [cited 2014 Dec 9];105(34):12569–74. Available from: http://www.pubmedcentral.nih.gov/articlerender.fcgi?artid=2527952&tool=pmcentrez&rendertype=abstract

Takagishi M, Chiba T. Efferent projections of the infralimbic (area 25) region of the medial prefrontal cortex in the rat: an anterograde tracer PHA-L study. Brain Res [Internet]. 1991 Dec 6 [cited 2015 May 27];566(1-2):26–39. Available from: http://www.ncbi.nlm.nih.gov/pubmed/1726062

Tononi G, Sporns O, Edelman GM. A measure for brain complexity: relating functional segregation and integration in the nervous system. Proc Natl Acad Sci [Internet]. 1994 May 24 [cited 2014 Sep 6];91(11):5033–7. Available from: http://www.pnas.org/content/91/11/5033.short

Uddin LQ, Supekar KS, Ryali S, Menon V. Dynamic reconfiguration of structural and functional connectivity across core neurocognitive brain networks with development. J Neurosci [Internet]. 2011 Dec 14 [cited 2014 Aug 23];31(50):18578–89. Available from: http://www.pubmedcentral.nih.gov/articlerender.fcgi?artid=3641286&tool=pmcentrez&rendertype=abstract

Vertes RP. Differential projections of the infralimbic and prelimbic cortex in the rat. Synapse [Internet]. 2004 Jan [cited 2014 Aug 29];51(1):32–58. Available from: http://www.ncbi.nlm.nih.gov/pubmed/14579424

Vesna Vuksanovic, Mario Bartolo, Dave Hunter LSAT. Frontiers: fMRI based Granger causality as a measure of effective connectivity in macaque visual cortex [Internet]. Front. Comput. Neurosci. Conf. Abstr. BC11 Comput. Neurosci. Neurotechnology Bernstein Conf. Neurex Annu. Meet. 2011. 2011 [cited 2014 Sep 6]. Available from: http://www.frontiersin.org/10.3389/conf.fncom.2011.53.00200/event_abstract

Vincent JL, Patel GH, Fox MD, Snyder AZ, Baker JT, Van Essen DC, et al. Intrinsic functional architecture in the anaesthetized monkey brain. Nature [Internet]. 2007 May 3 [cited 2014 Jul 13];447(7140):83–6. Available from: http://dx.doi.org/10.1038/nature05758

Vogt BA, Paxinos G. Cytoarchitecture of mouse and rat cingulate cortex with human homologies. Brain Struct Funct [Internet]. 2014 Jan [cited 2015 Jul 8];219(1):185–92. Available from: http://www.ncbi.nlm.nih.gov/pubmed/23229151

W. Liao, D. Marinazzo, Z. Pan HC. Kernel Granger Causality Mapping Effective Connectivity: A Resting fMRI Study,Advances in Cognitive Neurodynamics (II) [Internet]. Wang R, Gu F, editors. Dordrecht: Springer Netherlands; 2011 [cited 2014 Sep 2]. Available from: http://www.springerlink.com/index/10.1007/978-90-481-9695-1

Wen X, Rangarajan G, Ding M. Is Granger causality a viable technique for analyzing fMRI data? Zang Y-F, editor. PLoS One [Internet]. Public Library of Science; 2013 Jan [cited 2014 Aug 28];8(7):e67428. Available from: http://www.pubmedcentral.nih.gov/articlerender.fcgi?artid=3701552&tool=pmcentrez&rendertype=abstract

Wiener N. The theory of prediction. In: Beckenbach, E.F. (Ed.), Modern Mathematics for Engineers., New York (Chapter 8), [Internet]. McGraw-Hill. 1956 [cited 2014 Oct 13]. Available from:

http://www.cs.berkeley.edu/~zadeh/papers/1950-An Extension of Wieners Theory of Prediction.pdf

Wu G, Liao W, Stramaglia S, Ding J-R, Chen H, Marinazzo D. A blind deconvolution approach to recover effective connectivity brain networks from resting state fMRI data. Med Image Anal [Internet]. 2013a Apr [cited 2014 Jul 26];17(3):365–74. Available from: http://www.ncbi.nlm.nih.gov/pubmed/23422254

Wu G, Liao W, Stramaglia S, Marinazzo D. Recovering directed networks in neuroimaging datasets using partially conditioned Granger causality. BMC Neurosci [Internet]. 2013b [cited 2015 Apr 23];14(Suppl 1):P260. Available from: http://www.biomedcentral.com/1471-2202/14/S1/P260

Wu G-R, Liao W, Stramaglia S, Chen H, Marinazzo D. Recovering directed networks in neuroimaging datasets using partially conditioned Granger causality. Brain Connect [Internet]. 2013c Jan [cited 2014 Sep 5];3(3):294–301. Available from: http://www.pubmedcentral.nih.gov/articlerender.fcgi?artid=3685317&tool=pmcentrez&rendertype=abstract

Wu G-R, Stramaglia S, Chen H, Liao W, Marinazzo D. Mapping the voxel-wise effective connectome in resting state FMRI. PLoS One [Internet]. 2013d Jan [cited 2014 Sep 5];8(9):e73670. Available from: http://www.pubmedcentral.nih.gov/articlerender.fcgi?artid=3771991&tool=pmcentrez&rendertype=abstract

Wu X, Li R, Fleisher AS, Reiman EM, Guan X, Zhang Y, et al. Altered default mode network connectivity in Alzheimer's disease--a resting functional MRI and Bayesian network study. Hum Brain Mapp [Internet]. 2011 Nov [cited 2015 May 15];32(11):1868–81. Available from: http://www.pubmedcentral.nih.gov/articlerender.fcgi?artid=3208821&tool=pmcentrez&rendertype=abstract

Wu X, Yu X, Yao L, Li R. Bayesian network analysis revealed the connectivity difference of the default mode network from the resting-state to task-state. Front Comput Neurosci [Internet]. 2014 Sep 24 [cited 2014 Oct 1];8(September):1–9. Available from: http://www.frontiersin.org/Computational_Neuroscience/10.3389/fncom.2014.00118/abstract

Zhan Y, Paolicelli RC, Sforazzini F, Weinhard L, Bolasco G, Pagani F, et al. Deficient neuron-microglia signaling results in impaired functional brain connectivity and social behavior. Nat Neurosci [Internet]. Nature Publishing Group, a division of Macmillan Publishers Limited. All Rights Reserved.; 2014 Mar [cited 2014 Jul 10];17(3):400–6. Available from: http://dx.doi.org/10.1038/nn.3641

Zhang D, Snyder AZ, Fox MD, Sansbury MW, Shimony JS, Raichle ME. Intrinsic functional relations between human cerebral cortex and thalamus. J Neurophysiol [Internet]. 2008 Oct [cited 2014 Sep 6];100(4):1740–8. Available from: http://www.pubmedcentral.nih.gov/articlerender.fcgi?artid=2576214&tool=pmcentrez&rendertype=abstract

Zhou Z, Ding M, Chen Y, Wright P, Lu Z, Liu Y. Detecting directional influence in fMRI connectivity analysis using PCA based Granger causality. Brain Res [Internet]. NIH Public Access; 2009 Sep 15 [cited 2014 Sep 6];1289:22–9. Available from: http://www.pubmedcentral.nih.gov/articlerender.cgi?accid=PMC2730503

Zhou Z, Wang X, Klahr NJ, Liu W, Arias D, Liu H, et al. A conditional Granger causality model approach for group analysis in functional magnetic resonance imaging. Magn Reson Imaging [Internet]. Elsevier Inc.; 2011 Apr [cited 2014 Aug 30];29(3):418–33. Available from: http://www.pubmedcentral.nih.gov/articlerender.fcgi?artid=3063394&tool=pmcentrez&rendertype=abstract

Zhuang J, Peltier S, He S, LaConte S, Hu X. Mapping the connectivity with structural equation modeling in an fMRI study of shape-from-motion task. Neuroimage [Internet]. 2008 Aug 15 [cited 2014 Sep 6];42(2):799–806. Available from: http://www.sciencedirect.com/science/article/pii/S1053811908006691

Zingg B, Hintiryan H, Gou L, Song MY, Bay M, Bienkowski MS, et al. Neural networks of the mouse neocortex. Cell [Internet]. Elsevier; 2014 Feb 27 [cited 2014 Jul 10];156(5):1096–111. Available from: http://www.cell.com/article/S0092867414002220/fulltext